2019-12

OPTIMIZATION OF MULTI-JUNCTION SOLAR CELL FOR SPACE APPLICATIONS MODELED WITH RUBY, MATLAB, AND SILVACO

Allen, Tony Jr.

Monterey, CA; Naval Postgraduate School

NAVAL POSTGRADUATE SCHOOL

MONTEREY, CALIFORNIA

THESIS

OPTIMIZATION OF MULTI-JUNCTION SOLAR CELL FOR SPACE APPLICATIONS MODELED WITH RUBY, MATLAB, AND SILVACO

by

Tony Allen Jr.

December 2019

Thesis Advisor:	Sherif N. Michael
Second Reader:	Matthew A. Porter

THIS PAGE INTENTIONALLY LEFT BLANK

REPORT DOCUMENTATION PAGE			*Form Approved OMB No. 0704-0188*
Public reporting burden for this collection of information is estimated to average 1 hour per response, including the time for reviewing instruction, searching existing data sources, gathering and maintaining the data needed, and completing and reviewing the collection of information. Send comments regarding this burden estimate or any other aspect of this collection of information, including suggestions for reducing this burden, to Washington headquarters Services, Directorate for Information Operations and Reports, 1215 Jefferson Davis Highway, Suite 1204, Arlington, VA 22202-4302, and to the Office of Management and Budget, Paperwork Reduction Project (0704-0188) Washington, DC 20503.			
1. AGENCY USE ONLY ***(Leave blank)***	**2. REPORT DATE** December 2019	**3. REPORT TYPE AND DATES COVERED** Master's thesis	
4. TITLE AND SUBTITLE OPTIMIZATION OF MULTI-JUNCTION SOLAR CELL FOR SPACE APPLICATIONS MODELED WITH RUBY, MATLAB, AND SILVACO			**5. FUNDING NUMBERS**
6. AUTHOR(S) Tony Allen Jr.			
7. PERFORMING ORGANIZATION NAME(S) AND ADDRESS(ES) Naval Postgraduate School Monterey, CA 93943-5000			**8. PERFORMING ORGANIZATION REPORT NUMBER**
9. SPONSORING / MONITORING AGENCY NAME(S) AND ADDRESS(ES) N/A			**10. SPONSORING / MONITORING AGENCY REPORT NUMBER**
11. SUPPLEMENTARY NOTES The views expressed in this thesis are those of the author and do not reflect the official policy or position of the Department of Defense or the U.S. Government.			
12a. DISTRIBUTION / AVAILABILITY STATEMENT Approved for public release. Distribution is unlimited.			**12b. DISTRIBUTION CODE** A

13. ABSTRACT (maximum 200 words)

The purpose of this research is to document further research into the optimization techniques investigated by James Walsh and applied to Multi-junction Solar Cells. Walsh performed his research with the Near Orthogonal Latin Hypercube (NOLH) in order to optimize the design specifications for each layer of solar cell thickness and doping concentration. Walsh at the same time evaluated cell performance under the radiation effects of the space environment. This research performed a similar analysis, except for the radiation effects, but focused more on producing an algorithm that could be executed from single user input and significantly reducing the selected design space. This research produced an efficient program that seamlessly operates between Ruby, MATLAB, and Silvaco ATLAS in order to produce an optimal designed dual-junction solar cell for space applications, in a much smaller design space than the technique utilized by Walsh.

14. SUBJECT TERMS space solar cells, radiation effects, photovoltaic modeling, efficiency, optimization			**15. NUMBER OF PAGES** 107
			16. PRICE CODE
17. SECURITY CLASSIFICATION OF REPORT Unclassified	**18. SECURITY CLASSIFICATION OF THIS PAGE** Unclassified	**19. SECURITY CLASSIFICATION OF ABSTRACT** Unclassified	**20. LIMITATION OF ABSTRACT** UU

NSN 7540-01-280-5500 Standard Form 298 (Rev. 2-89) Prescribed by ANSI Std. 239-18

THIS PAGE INTENTIONALLY LEFT BLANK

OPTIMIZATION OF MULTI-JUNCTION SOLAR CELL FOR SPACE APPLICATIONS MODELED WITH RUBY, MATLAB, AND SILVACO

Tony Allen Jr.
Captain, United States Marine Corps
BSEE, University of North Florida, 2013

Submitted in partial fulfillment of the
requirements for the degree of

MASTER OF SCIENCE IN ELECTRICAL ENGINEERING

from the

NAVAL POSTGRADUATE SCHOOL
December 2019

Approved by: Sherif N. Michael
Advisor

Matthew A. Porter
Second Reader

Douglas J. Fouts
Chair, Department of Electrical and Computer Engineering

THIS PAGE INTENTIONALLY LEFT BLANK

ABSTRACT

The purpose of this research is to document further research into the optimization techniques investigated by James Walsh and applied to Multi-junction Solar Cells. Walsh performed his research with the Near Orthogonal Latin Hypercube (NOLH) in order to optimize the design specifications for each layer of solar cell thickness and doping concentration. Walsh at the same time evaluated cell performance under the radiation effects of the space environment. This research performed a similar analysis, except for the radiation effects, but focused more on producing an algorithm that could be executed from single user input and significantly reducing the selected design space. This research produced an efficient program that seamlessly operates between Ruby, MATLAB, and Silvaco ATLAS in order to produce an optimal designed dual-junction solar cell for space applications, in a much smaller design space than the technique utilized by Walsh.

THIS PAGE INTENTIONALLY LEFT BLANK

TABLE OF CONTENTS

THIS PAGE INTENTIONALLY LEFT BLANK

LIST OF FIGURES

LIST OF TABLES

THIS PAGE INTENTIONALLY LEFT BLANK

LIST OF ACRONYMS AND ABBREVIATIONS

AlAs	aluminum arsenide
AlGaAs	aluminum gallium arsenide
AlInP	aluminum indium phosphide
AlP	aluminum phosphide
GaP	gallium phosphide
Ge	germanium
GA	genetic algorithm
GaAs	gallium arsenide
InAlGaP	indium aluminum gallium phosphide
InGaP	indium gallium phosphate
InP	indium phosphide
NOLH	nearly orthogonal Latin hypercube
NPS	Naval Postgraduate School
NREL	National Renewable Energy Laboratory

THIS PAGE INTENTIONALLY LEFT BLANK

ACKNOWLEDGMENTS

I would like to show appreciation for the Naval Postgraduate School staff members who helped me in my research efforts: my thesis advisor, Professor Sherif Michael, my second reader, Matthew Porter, and Susan Sanchez from the Department of Operations Research.

I would also like to thank my wife, Latoya, my children, Essence, Elisha, and Tony, and my mother-in-law, Angela, for their support and patience during this time.

THIS PAGE INTENTIONALLY LEFT BLANK

I. INTRODUCTION

A. SOLAR CELLS FOR SPACE APPLICATIONS

Power sources for space craft may include batteries, both electric and chemically fueled engines, and photovoltaic systems onboard the craft. It is necessary for the design of these systems to be dependable and capable of surviving the harsh environment of space. Photovoltaic systems, or solar cells, have proven to be dependable in supplying spacecraft systems with the power they require. The cost of producing state-of-the-art multi-junction solar cells usually prohibits their use for terrestrial applications; however, multi-junction solar cells are vital for the survivability and success of space systems. For space applications, higher-cost multi-junction solar cells are preferred over the cheaper terrestrial solar cell variants due to their ability to withstand the harsh environment of space. Additionally, improving the efficiency in solar panel design will result in less of an electrical load required for solar power generation, a reduced surface area to prevent collision with orbital debris, and improve the capability to meet higher power demands.

The inspection of solar cell characteristics such as doping concentrations and material thicknesses make designing optimal cell parameters an immense task. The utilization of complex computer software that executes numerical approximation in order to solve nonlinear sets of differential equations while simultaneously modeling solar cell operation, are fundamental towards simulating the efficiency of theorized solar cell designs with precise parameters. Design improvements can be achieved by simulating solar cells with variants of the parameters listed above. Inspecting large numbers of simulation results provides a better observation of what parameter values result in the highest efficiency of the respective cell at a fraction of the cost of manufacturing countless solar cells with different characteristics.

B. PAST WORK AT NPS

Numerous theses have researched solar cell optimization at the Naval Postgraduate School (NPS). James Walsh [1] successfully modeled and simulated radiation effects on dual-junction cells under AM0 conditions. Panayiotis Michalopoulos [2] successfully implemented the modeling of several solar cells using Silvaco ATLAS (Silvaco), by demonstrating the performance of modeled cells and tested cells while studying their individual solar cell efficiency. Finally, both Raymond Kilway [3] and Silvio Pueschel [4] continued the work of P. Michalopoulos by researching the ability to optimize solar cell design by performing either a genetic algorithm (GA) or nearly orthogonal Latin hypercubes (NOLH), respectively. NOLH proved to be the more efficient method due to the length of time required to derive an optimized design and remains the method executed during the conduct of the research described here.

C. OBJECTIVE

The goal of this research is to inspect the solution space derived from the NOLH. J. Walsh investigated a solution space of more than 2,000 points for thicknesses and doping concentrations, discussed later in Chapter III. First, the published results of a simulated and manufactured dual-junction solar cell was utilized to derive the respective thicknesses and doping concentrations as the model for this research. Next, parameters were precisely determined to produce a scalable and realistic design space focusing mainly on the thicknesses and doping concentrations for the respective layers present in the dual-junction cell. Finally, parameters for binary, ternary, and quaternary materials were heavily utilized and calculated with MATLAB for use for the final design simulated in Silvaco ATLAS. To discuss the modeled solar cell researched more in depth, this research will converse a dual-junction indium gallium phosphate (InGaP)/gallium arsenide (GaAs) cell fabricated and tested at The Ohio State University [4]. This dual-junction solar cell provides tangible results to compare the produced simulated results.

D. ORGANIZATION

In Chapter II, the physics of semiconductors, solar cells, and multi-junction solar cells will be discussed. Chapter III will discuss the methodology of research and optimization techniques utilized with Silvaco ATLAS, MATLAB, and the NOLH algorithm. Chapter IV will discuss and list the results of the simulation presented throughout this research. Finally, Chapter V will discuss the conclusion, areas of future improvements, and recommended future work.

II. BACKGROUND

A. SEMICONDUCTORS

Semiconductor optimal performance is achieved only when the respective material can be grown with a high fidelity of crystallinity, while at the same time the impurities and defects can be regulated. In order to maintain exceptional structural attributes in the semiconductor design, a high-quality substrate must be available. Consequently, this requires growing crystals in bulk, which are then sliced and polished to allow epitaxial growth of thin regions within the semiconductor including heterostructures.

1. Energy Bands and Charge Carriers

There are two energy bands for electrons in a semiconductor, the conduction band and the valence band. The conduction band is the band of energies higher than the bandgap, and the valence band is the band of energies below the bandgap. Both energy bands possess particles that enable current flow; the conduction band maintains states of electrons and the valence band maintains holes. Whenever the conduction band possesses an empty state of an electron, a hole from the valence band travels to the conduction band to occupy this empty state. The band gap structure of a semiconductor material is revealed in Figure 1 [1].

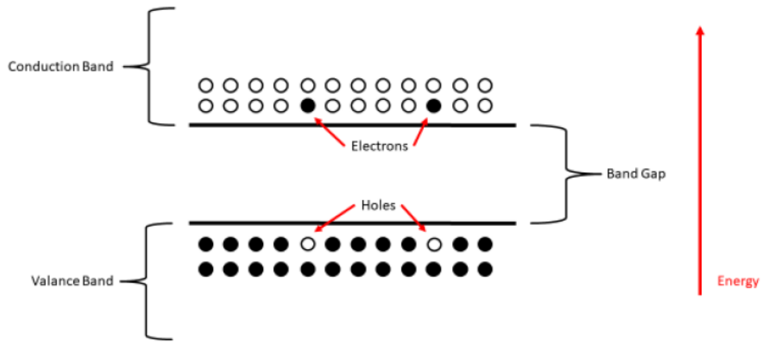

Figure 1. Bandgap structure for a semiconductor material. Source: [1].

Momentum, k, defines the shape of both the valence and conduction bands in respect to the band gap. This shape can depict the characteristic of direct bandgap material or indirect bandgap material. A direct bandgap material has the characteristic that the lowest energy point of the conduction band apportions momentum with the highest energy point on the valence band. The indirect bandgap material possesses a less efficient momentum counteracted between these two energy points. The bandgap materials and their respective energies are revealed in Figure 2 [5].

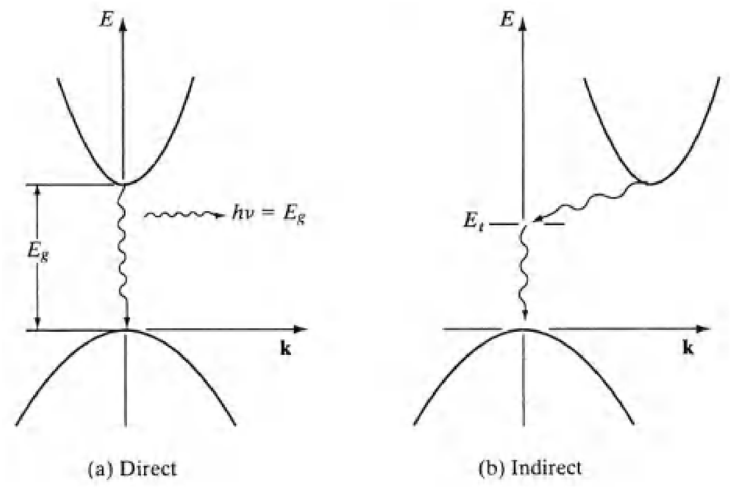

Figure 2. Direct and Indirect electron transitions in semiconductors. Source: [5].

The simple two-dimensional representation shown in Figure 2 is more problematic than simply described [1]. Figure 3 discloses the characteristic of silicon possessing a centered bandgap between the valence and conduction bands, versus the germanium arsenide bandgap. The band structures and energy dependent affinities will be discussed more in depth in Chapter III, Section C. Referring to Figure 2, the energy band curvature directly impacts the rate of momentum that also clearly impacts the rest mass of an electron or hole, and eventually the carrier mobility through a semiconductor [5].

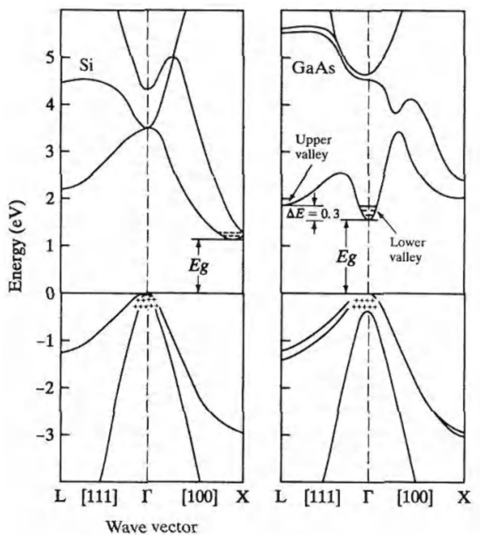

Figure 3. Real band diagram for Si and GaAs. Source: [5].

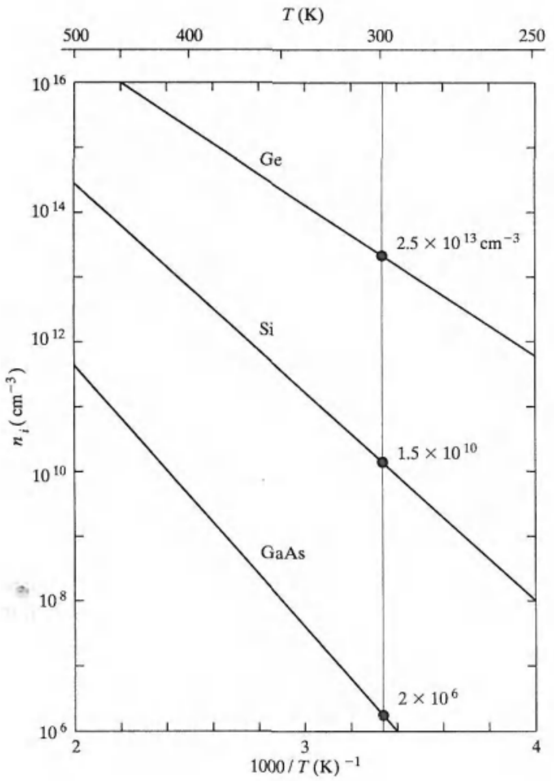

Figure 4. Intrinsic carrier concentration. Source: [5].

Figure 4 exposes the theoretical intrinsic carrier concentration for germanium, silicon, and gallium arsenide. It should be observed that these concentrations are plotted as a function of inverse temperature and room temperature values are indicated for reference. The intrinsic concentration can be calculated simply by the product of both the electron concentration n_o, and hole concentration p_o, of a material. This is revealed in Equation (1) [5].

$$n_o \, p_o = n_i^2 \tag{1}$$

Next, the Fermi-level will be discussed and its relation to the generation and recombination of electron hole pairs. The fermi-level should be understood as either possessing its location in the upper or lower parts of the bandgap. The differences between n-type and p-type materials in relation to filled states and their fermi-level are shown in Figure 5. The n-type material possesses a fermi-level above the bandgap and vice-versa for p-type material. N-type material is known to be a donor material N_D^+, and p-type material is known as an acceptor material N_A^-. The n-type material possesses filled states, electrons, in the conduction band E_C, and the p-type material possesses filled states, holes, in the valence band E_V.

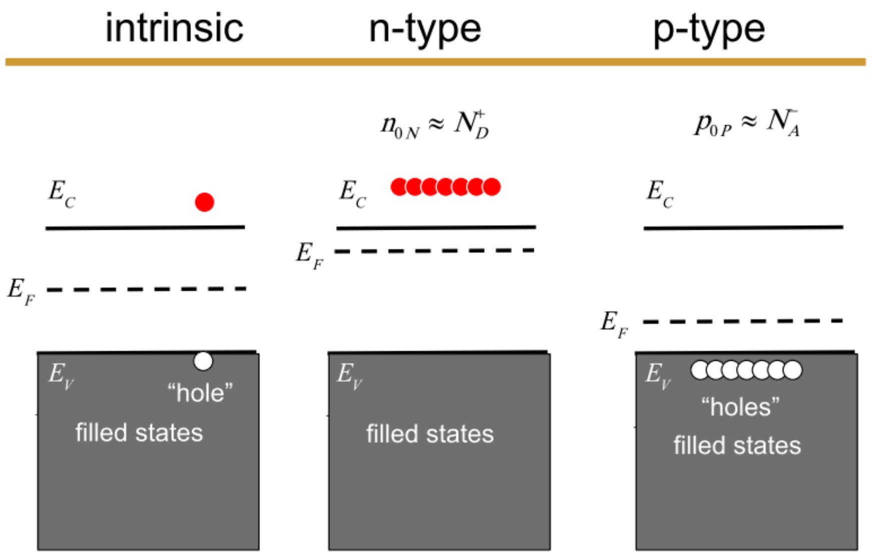

Figure 5. Filled states and Fermi-levels. Source: [6].

The fermi-function (Equation 2) is tied to Figure 5 for reference [5]. This was referenced to assist in better understanding the relationship of the fermi-level to the carrier concentrations present in the p-type or n-type specific materials. These n-type and p-type materials are the building blocks for PN junction semiconductors and will be discussed in the next paragraph.

$$f(E) = \frac{1}{1+ e^{(E-E_F)/kT}} \tag{2}$$

$$n = N_D e^{(E_F - E_C)/kT} \tag{3}$$

$$p = N_A e^{(E_V - E_F)/kT} \tag{4}$$

Equations (3) and (4) reveal the relationships that are shared between the fermi-levels, electron carrier concentration, and hole concentrations of the material and how the fermi-level directly impacts both carriers [5].

2. Semiconductor Materials and Doping Concentrations

When selecting elements to utilize for the construction of a semiconductor from the periodic table, silicon, a Group IV element, is chosen due to its relative purity. Figure 6 reveals the intrinsic silicon that is very pure, and containing a tiny amount of impurities [7]. Furthermore, every silicon atom is shown sharing its four valence electrons along with four neighboring atoms.

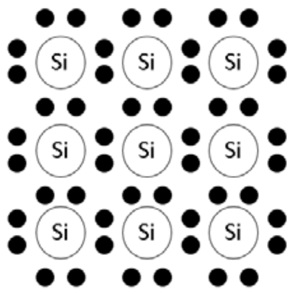

Figure 6. Intrinsic Si with no impurity. Source: [7].

Next, the doping of a semiconductor with either donor or acceptor impurities, also changes the band gap of the respective material [7]. It was explained that donor impurity changes donor level while an acceptor impurity changes the acceptor level [7]. Figure 7 reveals the effects of doping silicon with donor (phosphorous), thus making the silicon more negative and producing an n-type material of Si. Figure 8 reveals the opposite occurring with silicon when its doped with an acceptor (boron), thus producing a p-type material of Si. Finally, it must be understood that whenever a semiconductor is doped with different types of concentrations of impurities this varies the resistivity of the material.

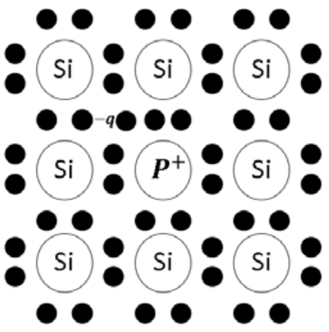

Figure 7. Silicon donor doped samples. Source: [7].

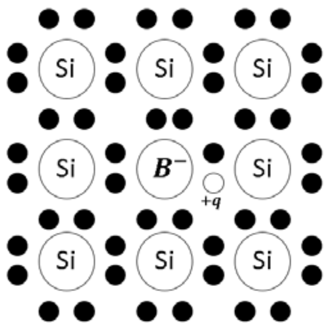

Figure 8. Silicon acceptor doped samples. Source: [7].

3. PN Junction

PN junctions are composed of N-doped semiconductor material and P-doped semiconductor material which are brought into contact with each other or manufactured in contact with each other. At the junction, a depletion region naturally forms when the N-doped and P-doped material is brought together, or manufactured together. The semiconductor material can be silicon, gallium, or a III-V compound semiconductor material such as GaAs. The key to a PN junction using any semiconductor material is that one side is doped N type while the other side is doped P type. Figure 9 illustrates the resulting energy band diagram for a PN semiconductor junction. Notice how the fermi-level E_F, is shown to possess the same level throughout the material, and the only change appears to be in the location in relation to either the valence band E_v or the conduction band E_c of the materials.

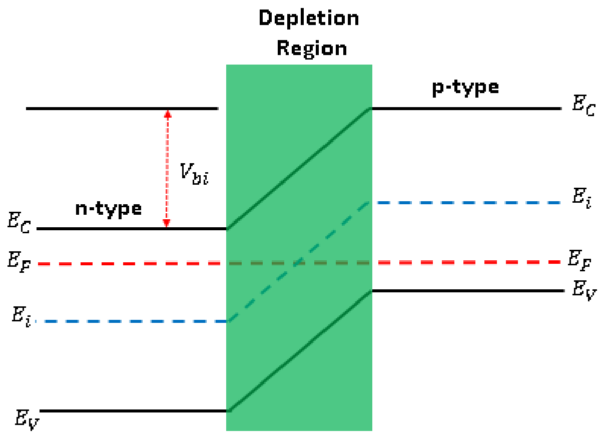

Figure 9. PN junction band diagram. Source: [6].

Figure 9 reveals the band structure of the PN junction while at equilibrium with no external electric field applied. Although no external electric field is applied to the PN junction, there is an internal electric field that exists between the n-type and p-type material with a built-in junction potential barrier existing as V_{bi}, thus producing the slope shown above. Both materials maintain their individual intrinsic levels, but the fermi level that exists between the two materials is not drawn to scale and has an approximate distance that’s relative to the intrinsic level shown above. Finally, the two materials create a depletion region where both electrons and holes are stationary in equilibrium as pictured in Figure 10. Take note of the placement of electrons and holes with the depletion region formed between the two materials. The electrons are positioned in the p-type material in the depletion region, and the holes are positioned in the n-type material in the depletion region waiting for a bias to initiate the diffusion and drift of carriers throughout the material.

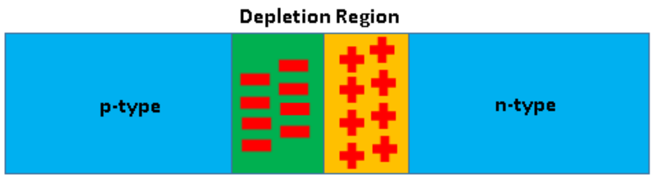

Figure 10. PN junction. Source: [5].

B.G. Streetman and S.K. Banerjee list the Poisson's equation (Equation 5) to provide a better idea of how the electric field distribution is mathematically modeled within the transition region. This transition region relates the gradient of the electric field in respect to the local space charge at any point $\boldsymbol{x}$ [5].

$$\frac{d\,\mathcal{E}(x)}{dx} = \frac{q}{\epsilon}\left(p - n + N_d^+ - N_a^-\right) \tag{5}$$

Poisson's equation can also be simplified within the transition upon neglecting the contribution of the carriers $(p - n)$ in respect to the space charge. The two regions of constant space charge resolve to the following equations [5].

$$\frac{d\,\mathcal{E}(x)}{dx} = \frac{q}{\epsilon} N_d, 0 < x < x_{n0} \tag{6}$$

$$\frac{d\,\mathcal{E}(x)}{dx} = -\frac{q}{\epsilon} N_a, -x_{p0} < x < 0 \tag{7}$$

Additionally, this relationship is only satisfied while assuming complete ionization of impurities $(N_d^+ = N_d)$ and $(N_a^- = N_a)$. The relation of the equations above allowed for the simplicity of relating the electric field to the contact potential V_o [5].

$$\mathcal{E}(x) = -\frac{d\,V(x)}{dx}\ or - V_o = \int_{-x_{p0}}^{x_{n0}} \mathcal{E}(x)dx \tag{8}$$

Next, Equation (9) relates the contact potential to the width of the depletion region.

$$V_o = -\frac{1}{2}\,\mathcal{E}_0\,W = \frac{1}{2}\,\frac{q}{\epsilon}N_d x_{n0}\,W = \frac{1}{2}\frac{q}{\varepsilon}\frac{N_a\,N_d}{N_a + N_d}W^2 \tag{9}$$

Finally, Equation (10) reveals the resulting solution for width of the depletion region in respect to the n-type and p-type materials, individual doping concentrations, and shared initial contact potential.

$$W = \sqrt{\frac{2\epsilon V_0}{q} \frac{N_a + N_d}{N_a\, N_d}} \tag{10}$$

4. Generation Rate and Recombination

B.G. Streetman and S.K. Banerjee explain the process of generation and recombination of electron-hole pairs within a semiconductor. This effect is achieved by the material absorbing photons with energy greater than the band gap while balanced by direct or indirect recombination [5]. Figure 11 illustrates this occurrence more simply. It should be observed that the energy of the light, or a photon, entering the material is greater than the bandgap energy that generates electron hole pairs in the existing material. This phenomenon likewise occurs with similar energies that have the capability of penetrating the material and having this same effect on the bandgap of the material.

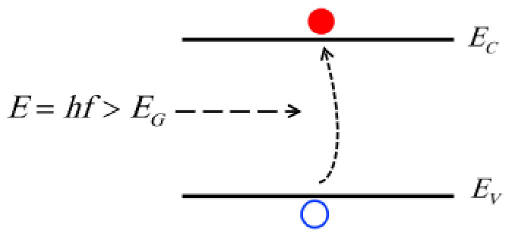

Figure 11. Light generating electron-hole pairs. Source: [6].

Next, the momentum discussed in paragraph 1 will be further discussed with its effect on the generation and recombination of electron hole pairs in a semiconductor. In a semiconductor, an intrinsic concentration, n_i, of electrons or holes exist, and this

occurs from the thermal generation-recombination between the valence band and conduction band. Additionally, adding energy to this material creates more of these particles in its respective material. Energy in the form of increasing temperature, an electric field, or photons can affect the intrinsic concentration of the material. Finally, for every electron that travels to the conduction band, it leaves behind a hole in its original position (Figure 12) [1].

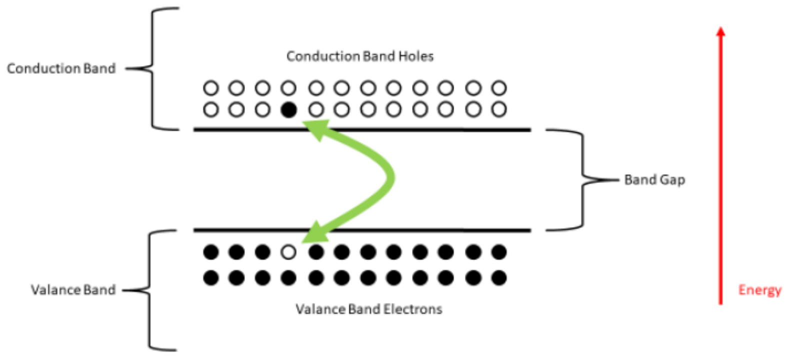

Figure 12. Electron promoted to conduction band. Source: [1].

B. SOLAR CELLS

1. Photodetectors and Photoconductors

S. M. Sze and K.K. Ng explain the concept of photodetectors and how they are a type of semiconductor device capable of detecting optical signals [7]. These authors further explain the fundamental concepts of a photodetector's operation and its three basic manners. However, the main characteristic observed in this research is the ability of the material to perform carrier generation once it is exposed to light [7]. Next, they further explain the two classes of photodetectors that exist today, in the form of thermal detectors and photon detectors. Thermal detectors are used to detect light more towards the far-infrared wavelength applications. Photon detectors are utilized in the application for use of absorbing visible light in order to generate a photocurrent. The photoelectric effect is known as a photon exciting a carrier that produces a photocurrent. The photoelectric effect is based on the photon energy hv and photon flux density and how they are both affected by the solar spectrum.

$$\lambda = \frac{hc}{\Delta E} = \frac{1.24}{\Delta \mathrm{E}\ (eV)}\ (\mu m) \tag{11}$$

Equation (11) reveals the relationship between the wavelength λ, the speed of light c, and the transition of energy levels ΔE [7]. The photon energy must possess the characteristic $h\nu > \Delta E$ in order to cause excitation associated with the minimum wavelength necessary for detection. Photon energy is also utilized to determine the quantum efficiency.

$$\eta = \frac{I_{ph}}{q\phi} = \frac{I_{ph}}{q}\left(\frac{h\nu}{P_{opt}}\right) \tag{12}$$

Next, the quantum efficiency is defined as the number of carriers produced per photon. Equation (12) provides the parameters needed to evaluate the quantum efficiency of a photodetector. Besides observing the photon energy, the photocurrent I_{ph}, photon flux ϕ and the optical power P_{opt} are considered. S. M. Sze and K.K. Ng further explain with use of Figure 13 how industry uses the quantities listed in Equation (12) for deriving the efficiency to observe at different atmospheric conditions how the photon energy, wavelength, and photon flux are impacted [7]. AM0 are measured observations for space and AM1.5 is for terrestrial applications.

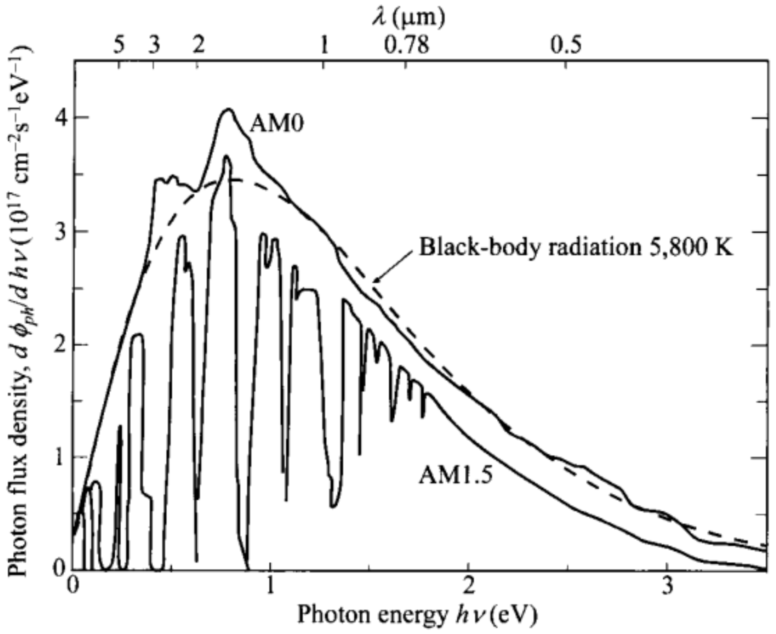

Figure 13. Solar Spectrum for AM0 and AM1.5. Source: [7].

2. Solar Cell Operation

S. M. Sze and K.K. Ng discuss considerations while designing solar cells and the three factors that exist for the optimal design. They declare high efficiency, inexpensive costs, and exceptional reliability are suited for an optimal design [7]. For example, crystal silicon solar cells are widely used with the best reported efficiency reaching higher than 22% [7]. Thin-filmed solar cells are desired for some applications due to their low-cost in processing and materials used. However, their disadvantages are poor efficiency and continuing instability. Thin-filmed solar cells have either single-junction or multi-junction cell structures. Multiple-junction cells have proven to possess higher efficiencies than single-junction cells, due to their different designs and configurations. Currently, three-junction cells designed with compound semiconductors of GaAs/InGaAs and InGaP/InGaAs/Ge have produced efficiencies higher than 30%, the highest of any structure [7]. M. Lundstrom discuss the concept of measuring efficiency of a solar cell, which can be simply focused on the short circuit current and the open circuit voltage [6]. He also explains the importance of the calculated fill factor of the solar cell to find the output power P_{out} [6]. Equations (13) and (14) are provided for reference.

$$P_{out} = I_{SC} V_{OC} FF \tag{13}$$

$$\eta = \frac{P_{out}}{P_{in}} = \frac{V_{oc} J_{sc} FF}{P_{in}} \tag{14}$$

$$FF = \frac{P_{out}}{V_{oc} J_{sc}} \tag{15}$$

The fill factor is determined by the diode characteristic and series resistances. The fill factor can also be simply analytically found as shown in Equation 15. The short circuit current is determined while the voltage is zero, the short circuit current is observed when the voltage is zero, and the fill factor is observed by integrating the area under the I-V curve in Figure 14, then dividing the result by the product of the short circuit current and the open circuit voltage [6].

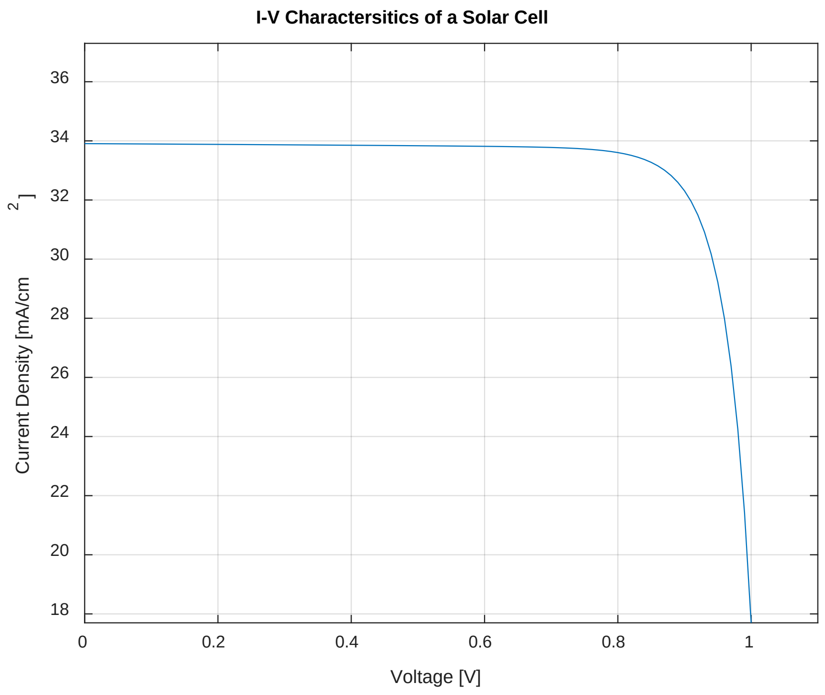

Figure 14. I-V characteristics for solar cell.

C. MULTI-JUNCTION SOLAR CELLS

1. Manufacturing

Multi-junction Solar Cells are known for being able to take advantage of the theoretical maximum efficiency by combining multiple layers of compound semiconductors together as discussed previously with GaAs/InGaAs and InGaP/InGaP/InGaAs/Ge. This was achieved by balancing the expected band gap for both the respective photocurrent and open-circuit voltage of the semiconductor. Additionally, efficiency is improved with photon absorption due to how the cells are arranged in their respective design that takes advantage of the lowest band gap present within the entire multi-junction design. These multi-junction cells are produced as thin-films [7].

2. Tunnel Junctions

S. M. Sze and K.K. Ng explain that tunnel diodes consist of simple p-n junctions that are heavily doped with impurities [7]. They further explain how tunnel junctions enable the tunneling process that allows electron tunneling from the valence band to the conduction band when a reverse bias is applied. Additionally, the tunneling process can either be direct or indirect.

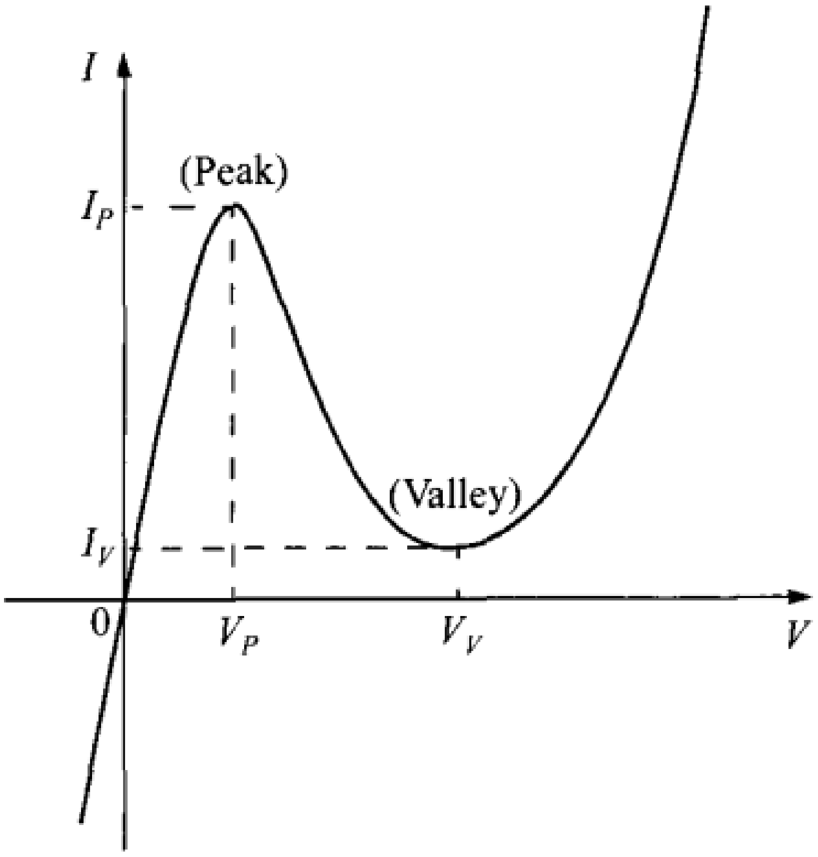

Figure 15. Static I-V characteristics of a tunnel diode. Source: [7].

Furthermore, they explain the behavior of the static current and voltage behavior of a tunnel diode in Figure 16. Both the peak and valley voltages and currents are shown for their static behavior [7].

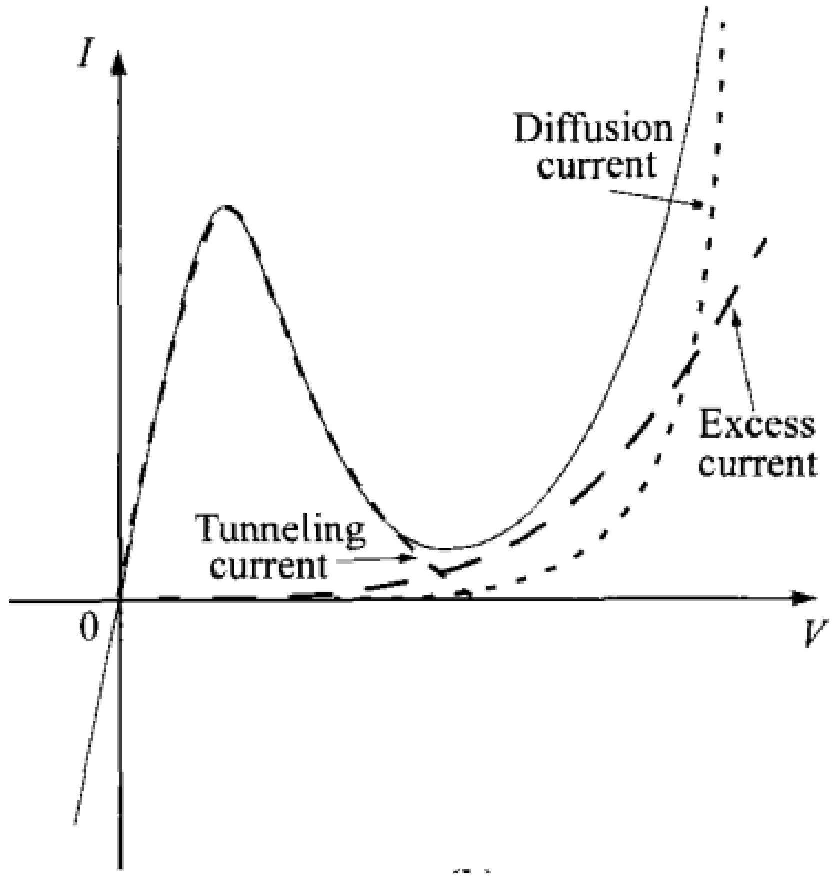

Figure 16. Three components of static characteristics. Source: [7].

Finally, S. M. Sze and K.K. Ng reveal the total static characteristics of the tunnel diode broken into three current components in Figure 16 [7]. The components are diffusion current, excess current, and tunneling current. They further explain the static characteristics at equilibrium. At equilibrium, it was explained that the tunneling current is the current that moves from the conduction band to an empty state in the valence band. Next, the excess current is caused by carrier tunneling this effect is caused by energy states that exist within a forbidden gap that appear in both the valence band and conduction band. Conclusively, diffusion current for a tunneling diode is what allows the actual current to flow between both materials present in the p-n junction.

THIS PAGE INTENTIONALLY LEFT BLANK

III. METHODOLOGY

A. MODELED CELL

The modeled cell simulated in this research is a dual-junction InGaP-GaAs cell fabricated at The Ohio State University [8]. This dual-junction cell was chosen due to the properties of each layer thickness, composition, and doping concentration, which is shown in Figure 17. The cell performance measurements are listed in Table 1 [8]. Although based partly on assumptions, the model was validated by comparing simulation output against provided data. The modeled cell overall structure and composition will be discussed next.

The very top of the cell has a contact layer that is made of GaAs, and the buffer layer is constructed from the same material. The dual junction cell is grown on a germanium (Ge) buffer and a silicon germanium (SiGe) substrate. Lueck et al. supplied the structure design shown in Figure 17 that reveals the arrangement of the modeled dual-junction cell [8].

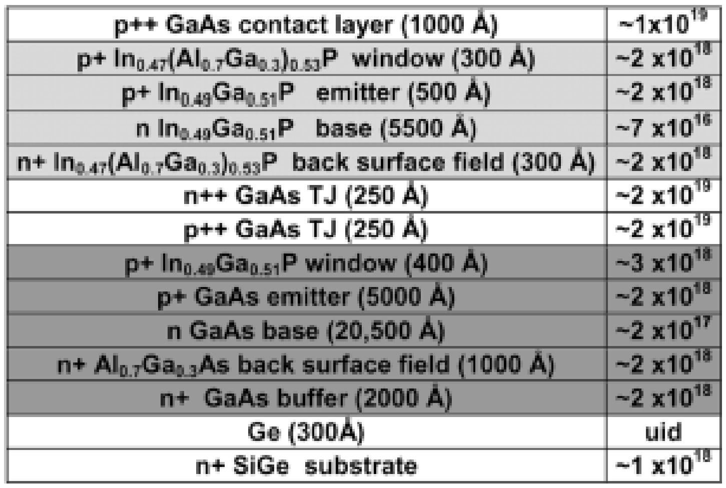

p++ GaAs contact layer (1000 Å)	~1x10^{19}
p+ $In_{0.47}(Al_{0.7}Ga_{0.3})_{0.53}P$ window (300 Å)	~2 x10^{18}
p+ $In_{0.49}Ga_{0.51}P$ emitter (500 Å)	~2 x10^{18}
n $In_{0.49}Ga_{0.51}P$ base (5500 Å)	~7 x10^{16}
n+ $In_{0.47}(Al_{0.7}Ga_{0.3})_{0.53}P$ back surface field (300 Å)	~2 x10^{18}
n++ GaAs TJ (250 Å)	~2 x10^{19}
p++ GaAs TJ (250 Å)	~2 x10^{19}
p+ $In_{0.49}Ga_{0.51}P$ window (400 Å)	~3 x10^{18}
p+ GaAs emitter (5000 Å)	~2 x10^{18}
n GaAs base (20,500 Å)	~2 x10^{17}
n+ $Al_{0.7}Ga_{0.3}As$ back surface field (1000 Å)	~2 x10^{18}
n+ GaAs buffer (2000 Å)	~2 x10^{18}
Ge (300Å)	uid
n+ SiGe substrate	~1 x10^{18}

Figure 17. Modeled cell profile. Source: [8].

Both AM0 and AM1.5 illumination for both GaAs and SiGe are listed for the η, V_{OC}, J_{sc}, and FF in the paper, and are displayed in Table 1 [8]. However, for the conduct of this research only AM0 for GaAs will be discussed. These parameters are listed to reveal the overall performance of this modeled dual-junction cell. The total area efficiency for AM0 was recorded at 18.6% for the cell grown on a GaAs substrate with a V_{OC} of 2.34 V, J_{SC} of 13.08 mA/cm^2, and a FF of 82.5%. These measured quantities are also listed in Table 1, and they assisted in predicting favorable results between the modeled cell and any further simulated cells that were produced during this research.

Table 1. Lighted current voltage for GaAs. Source: [8].

	GaAs	
	AM0	**AM1.5G**
J_{SC} (mA/cm^2)	13.08	10.9
$V_{OC}(V)$	2.34	2.32
$FF(\%)$	82.5	79.0
$\eta(\%)$	18.6	20.0

Lueck et al. provided Figure 18 to illustrate the I-V characteristics of the performance for the modeled cell at both AM0 and AM1.5. The authors also noted that the measurements performed in Figure 18 were the results of AM0 and AM1.5 illumination of GaInP/GaAs dual-junction cells on GaAs and SiGe substrates. AM0 measurements were performed at the NASA Glenn Research Center, and the AM1.5G were performed at the National Renewable Energy Laboratory (NREL). The baseline performance for the GaAs substrate will be measurements recorded for AM0.

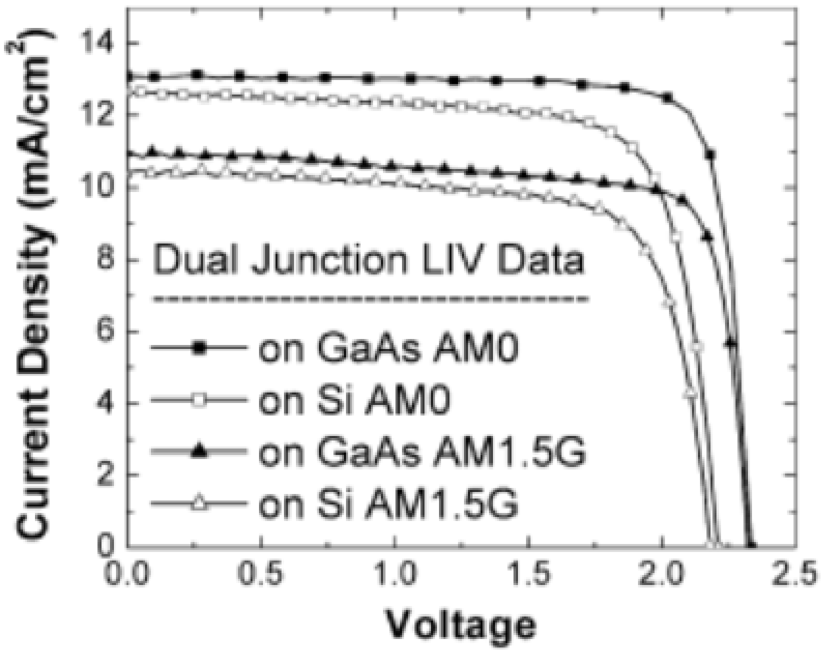

Figure 18. I-V measurements under AM0 and AM1.5G. Source: [8].

B. SILVACO ATLAS

Silvaco ATLAS is primarily used to model and simulate semiconductors in the semiconductor industry. Silvaco ATLAS was used heavily during this research to simulate the dual-junction cell. The baseline of the modeled cell depicted in the last section was first created to ensure accuracy of measurements before any further designs were introduced. Silvaco ATLAS enables the user to perform simulations for two-dimensional and three-dimensional semiconductors. Silvaco ATLAS possesses its own scripting language for the designed semiconductor device to be tested. If Silvaco ATLAS is executed properly, the result will be as shown in Figure 19.

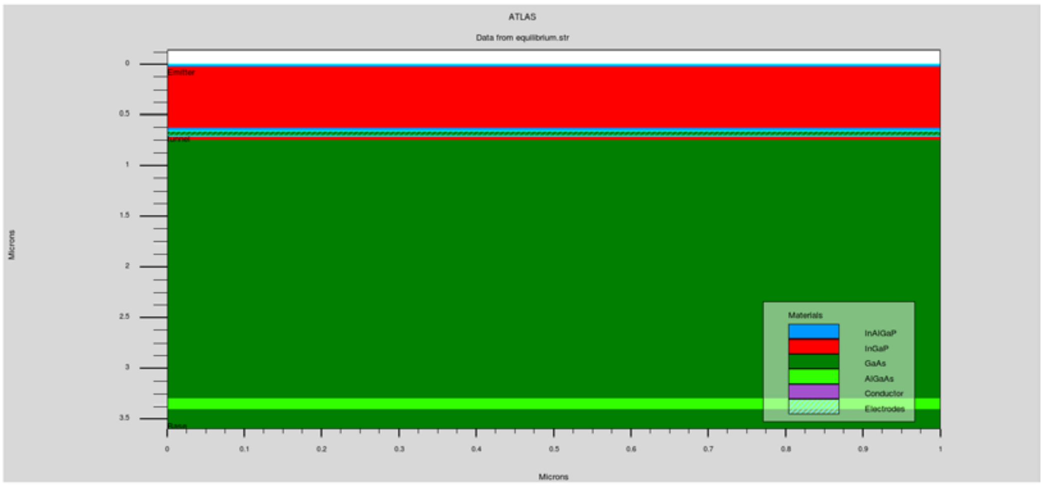

Figure 19. Modeled cell created in Silvaco

In order to ensure the correct and efficient design of any semiconductor, the order of statements for the mesh definition, structural definition, and solution groups must be constructed. For the mesh definition that exist within a simulation the user must carefully allocate mesh nodes at their defined regions, especially at regions of high activity. The mesh definition ensures that the simulated design space will perform as designed. This definition also directly affects the generation and recombination of electron-hole pairs throughout the entirety of the structure. The structural definitions ensure that every layer of material is precisely placed according the thickness and doping concentration specified in the design. The top section, tunneling junction, bottom section, and electrodes are depicted in Figure 19. Finally, the solution groups were important to ensure the necessary data was available for analysis later in the research in order to determine the performance of each designed cell. The solutions utilized heavily throughout this research were solutions of the designed cell under forward biased conditions in order to extract the η, V_{OC}, J_{sc}, and FF .

C. MOBILITY

The ability of electrons and holes to travel through a material is known as electron mobility μ_n and hole mobility μ_p, respectively. The mobility of either of these carriers is utilized as a function of doping for binary materials and this function is even more complex for both ternary and quaternary materials. This is due to the complexities involved with the various doping concentrations of these materials. Walsh discussed in depth the modeling constants and mobility parameters for GaAs, GaP, AlAs, and AlP for calculating the approximate mobilities for use within Silvaco ATLAS [1]. The modeling constants and mobility parameters were used extensively to ensure the modeling that was previously utilized by Walsh remained consistent throughout the performance of this research. The individual MATLAB functions and associated values are listed in the Appendices F through I, L, and N.

D. NEARLY ORTHOGONAL LATIN HYPERCUBE

The purpose of utilizing NOLH is to ensure designs are produced with minimal correlations while finding nearly orthogonal designs. The use of NOLH is reinforced by the user observing the design space not prematurely limited. In addition, an optimal solution is based on a Latin hypercube design that possesses an orthogonal regression matrix that includes quadratics and two-way interactions [9].

Next, Table 2 reveals the implementation of a solution from NOLH. This spreadsheet supplied from the NPS Simulation, Experiments and Efficient Design (SEED) Center for Data Farming was helpful in understanding how NOLH produces results from user inputs. The user is required to supply the minimum limits, maximum limits, and desired decimal placement solution of the resulting matrix. It should be observed that the resulting solution provides nearly uncorrelated solutions for both thickness and doping concentration. The spreadsheet utilized in Table 2 was hard coded for 22 factors that provided up to 262 different results for each column of data.

Table 2. NOLH example

low level	**0.02**	**17**	**0.04**	**17**	**0.53**	**15**	**0.03**	**17**
high level	**0.04**	**19**	**0.05**	**19**	**0.56**	**17**	**0.05**	**19**
decimals	**3**	**3**	**3**	**3**	**3**	**3**	**3**	**3**
factor name	**thick**	**doping**	**thick**	**doping**	**thick**	**doping**	**thick**	**doping**
	0.025	17.891	0.044	17.906	0.54	16.375	0.041	18.516
	0.038	17.609	0.044	17.922	0.533	15.906	0.038	17.406
	0.029	18.516	0.04	17.547	0.542	15.313	0.045	18.297
	0.034	18.781	0.043	17.734	0.543	16.516	0.031	17.813
	0.02	17.781	0.046	17.469	0.533	16.063	0.037	18.859
	0.034	17.859	0.047	17.016	0.542	15.656	0.042	17.078
	0.028	19	0.048	17.578	0.535	15.453	0.035	18.875
	0.031	18.406	0.049	17.125	0.54	16.844	0.047	17.031
	0.02	17.094	0.043	17.406	0.536	16.953	0.045	17.859

Finally, NOLH provided a usable design space that delivered usable thickness and doping concentration data upon command for multiple designs. However, during this research another approach was utilized that did not require the use of spreadsheets. The Ruby program was recommended by the SEED Center and utilized to take full advantage of the design capabilities provided in NOLH. Ruby proved to be highly useful and accurate in developing more complicated design spaces on command.

IV. RESULTS

A. MODELED CELL

After collecting the published thicknesses and doping concentrations from the real cell, the next step was to produce a reliable model within Silvaco ATLAS. This step was necessary in order to baseline any further optimization trials. Figure 20 reveals the performance comparison between the real cell and the modeled cell.

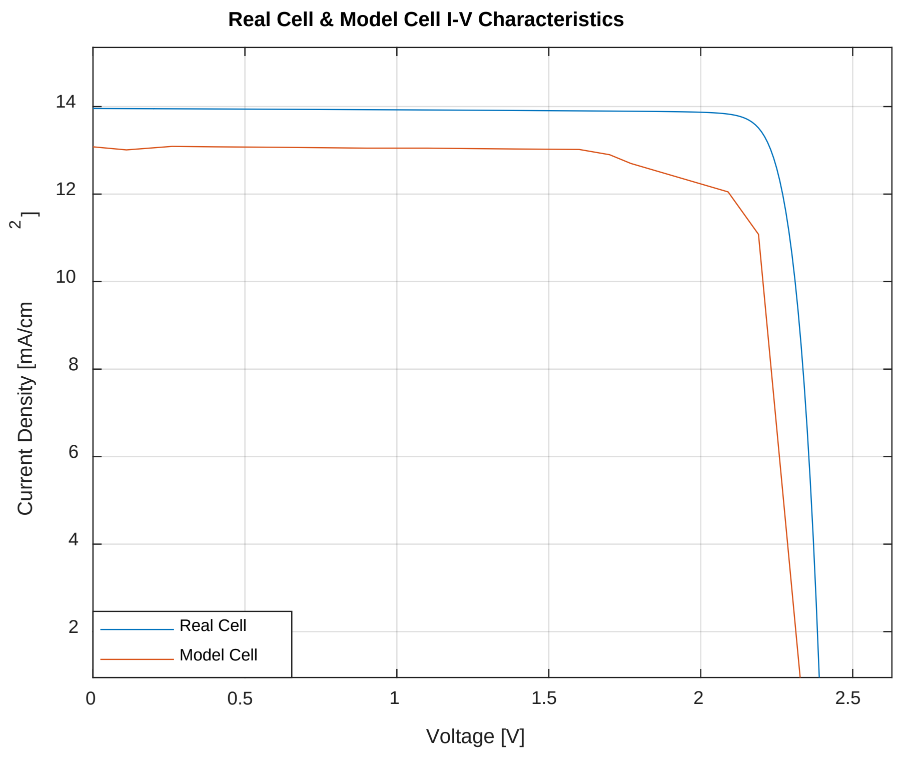

Figure 20. Comparison of real and modeled cell. Source: [8].

After plotting and comparing the real and modeled cell, the η, V_{OC}, J_{sc}, and FF were measured and compared to the real cell in Table 3. It was observed upon constructing the modeled cell that an error of 29% existed between the real cell and the modeled cell. It was determined that the error was due to how the tunnel junction was modeled for the simulation. The modeled tunnel junction was built with a high resistance placed in series with an electrode in the middle of the structure. This was the same procedure Walsh described in order to increase the speed of individual simulations in Silvaco ATLAS [1].

Table 3. Performance comparison of real and modeled cells

	Real	**Model**	**Error (%)**
η (%)	18.6	24.03	29.19
$V_{OC}(V)$	2.34	2.39	2.14
J_{SC} (mA/cm^2)	13.08	13.96	6.73
FF(%)	82.5	97.07	17.6

B. OPTIMIZATION RESULTS

The optimization runs consisted of three separate design spaces selected with NOLH. NOLH was called and executed by various different stack commands that provided the desired input for minimum and maximum values for Ruby to execute. Ruby also required specific stack commands to ensure a design space that consisted of 129, 257, and 385 design points. Each design space provided their respective number of designs to be executed. For example, the design space that consisted of 129 design points provided 129 different designs to be simulated at a time. The 129th design file created to be simulated in Silvaco ATLAS turned out to be the optimal design created out of the batch. However, the subsequent 257 and 385 design spaces provided optimal designs well within their respective design files created. The 205th design produced from the 257 design space was the most efficient. Likewise, the 216th design produced from the 385 design space was the most efficient in its respective design space. Figure 21 reveals the comparison of the modeled cell and all three optimal designs produced from each design space.

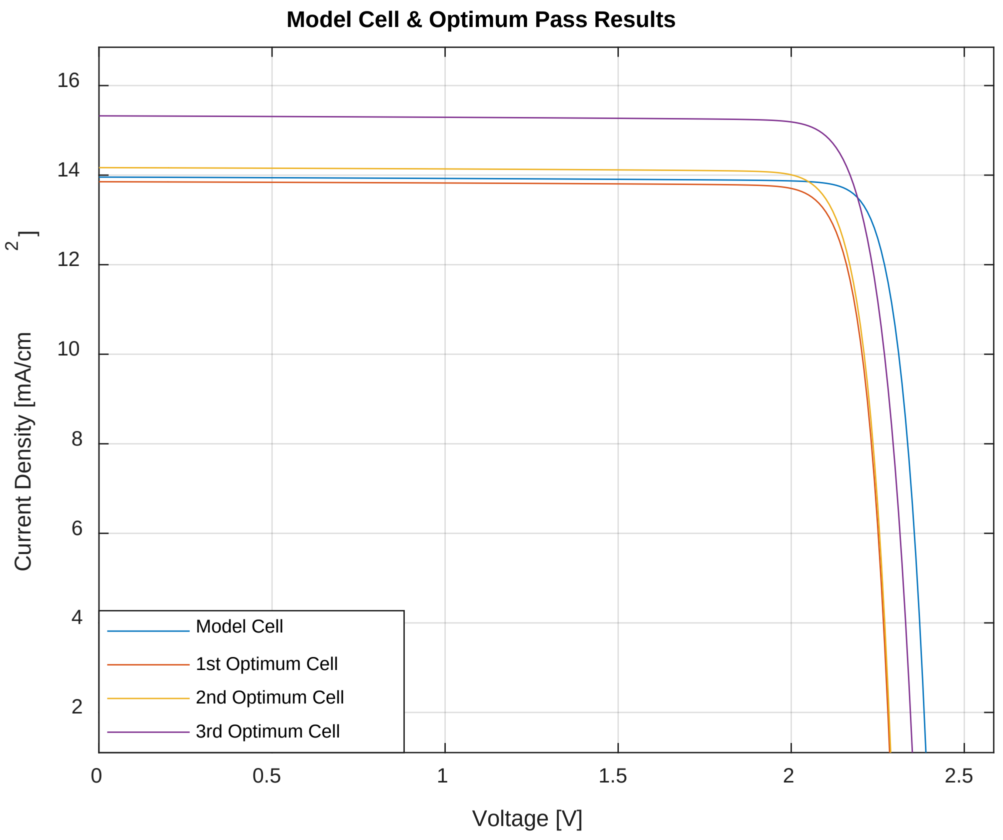

Figure 21. Comparison of model and optimization passes

Table 4 lists the parameters in terms of the η, V_{OC}, J_{sc}, and FF for each design space. It should be seen that even though each design space provided optimal performance for each of their respective design spaces, the 385th design space provided the first optimal design that surpassed the modeled cell.

Table 4. Optimization results

	Iteration	$\eta(\%)$	$V_{OC}(V)$	$J_{SC}\ (mA/cm^2)$	$FF(\%)$
Model	n/a	24.03	2.39	13.96	97.07
129 Design Points	129th	22.78	2.29	13.85	96.95
257 Design Points	205th	23.32	2.29	14.17	96.92
385 Design Points	216th	25.80	2.36	15.32	96.45

Table 5 reveals the overall improvements made from each optimization design pass. As stated earlier, the 385 design space in its 216th design provided the only improvement over the modeled cell.

Table 5. Model vs. optimization improvements

Design Points	$\boldsymbol{\eta}$ (%)	**Improvement**
Model	24.03	0.00%
129	22.78	-5.21%
257	22.32	-2.96%
385	25.80	7.34%

Table 6 lists the thicknesses and doping concentrations for the optimized design extracted from the 385 design space that provided a 7.34% improvement over the modeled cell. In addition to this improved design, this new optimized model would potentially provide a structure with an efficiency of 19.97%.

Table 6. Optimal designed dual-junction cell

Layer	**Thickness**	**Doping Concentration**
$In_{0.47}(Al_{0.7}Ga_{0.3})_{0.53}P$ (window) p+	0.02 μm	2.8e17 cm^{-3}
$In_{0.49}Ga_{0.51}P$ (emitter) p+	0.02 μm	2.2e18 cm^{-3}
$In_{0.49}Ga_{0.51}P$ (base) n	0.56 μm	7.8e16 cm^{-3}
$In_{0.47}(Al_{0.7}Ga_{0.3})_{0.53}P$ (back surface field) n+	0.01 μm	8.1e16 cm^{-3}
$GaAs$ (TJ) n++	0.025 μm	5e19 cm^{-3}
$GaAs$ (TJ) p++	0.025 μm	5e19 cm^{-3}
$In_{0.49}Ga_{0.51}P$ (window) p+	0.03 μm	2.5e17cm^{-3}
$GaAs$ (emitter) p+	0.52 μm	1.6e17cm^{-3}
$GaAs$ (base) n	2.05 μm	2.6e17 cm^{-3}
$Al_{0.7}Ga_{0.3}As$ (back surface field) n+	0.10 μm	4.7e18 cm^{-3}
$GaAs$ (buffer) n+	0.21 μm	2.4e17cm^{-3}

V. CONCLUSIONS AND FUTURE WORK

In conclusion, instead of performing an analysis for the largest design space Walsh could create from the spreadsheet he accessed from the SEED Center for Data Farming. It was theorized that the optimal design could be found from a smaller design space, resulting in faster optimization passes that could provide the same if not better results. Additionally, while pursuing this approach, it was determined that a more efficient process existed to execute NOLH without the necessity of manipulating the spreadsheet. Dr. Susan Sanchez from the NPS Operation Research department, was an exceptional resource in understanding how to utilize Ruby and applying the NOLH instructions in order to create the desired design space. Upon learning how to operate Ruby proficiently, the next task was to connect Ruby to MATLAB, and then MATLAB to Silvaco ATLAS. It was also pre-determined that the modeling of the tunnel junction would have to be simplified by placing a high resistance in series with an electrode in this region. This implementation still provided acceptable performance. Finally, for the seamless operation between MATLAB, Ruby, and Silvaco ATLAS, there were several functions that were built within MATLAB. These functions were the essential building blocks to ensure efficiency of commands that were easily executable.

Further research may focus on several areas. First, extending the functionality to optimize cell design by either material or fractional molar composition. Second, improvement of the tunnel junction modeling of the doping concentration or thickness. Third, perform a statistical analysis of the thicknesses and doping concentrations to optimize a single design space by utilizing the model to analyze and produce a new data set of values for the thicknesses and doping concentrations. There’s already a MATLAB function built and listed in Appendix Y to implement. Fourth, a further implementation to attempt to execute automation of the results as they are analyzed for efficiency. Fifth, the continuation of the investigation into the optimization of solar cells for the radiation environment of space.

THIS PAGE INTENTIONALLY LEFT BLANK

APPENDIX A. RUBY DOWNLOAD AND FAMILIARIZATION

First, Google "Ruby download" in order to find the associated web page below in Figure 22.

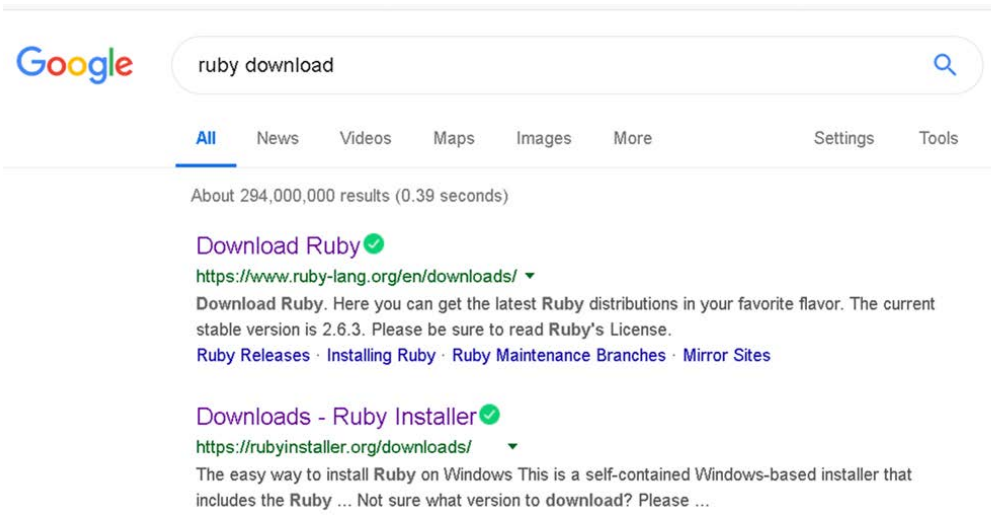

ruby download

All News Videos Maps Images More Settings Tools

About 294,000,000 results (0.39 seconds)

Download Ruby
https://www.ruby-lang.org/en/downloads/
Download Ruby. Here you can get the latest **Ruby** distributions in your favorite flavor. The current stable version is 2.6.3. Please be sure to read **Ruby's** License.
Ruby Releases · Installing Ruby · Ruby Maintenance Branches · Mirror Sites

Downloads - Ruby Installer
https://rubyinstaller.org/downloads/
The easy way to install **Ruby** on Windows This is a self-contained Windows-based installer that includes the **Ruby** ... Not sure what version to **download**? Please ...

Figure 22. A-1: Find Ruby Download. Source: [10].

Next, I downloaded " Ruby+Devkit 2.5.5-1 (x64)" compatible for my windows laptop, as shown in Figure 23.

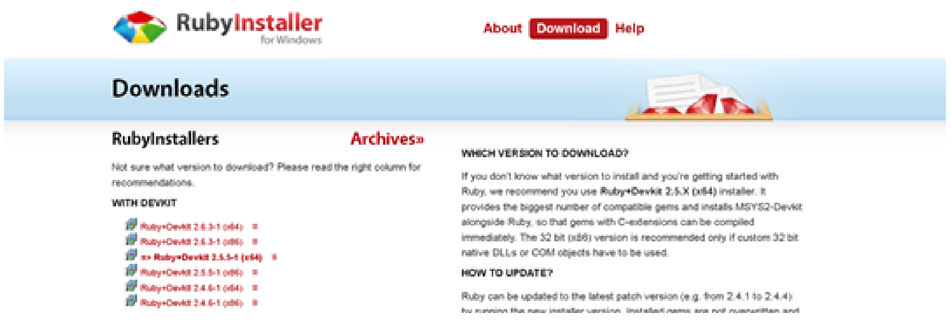

RubyInstaller for Windows

About Download Help

Downloads

RubyInstallers Archives»

Not sure what version to download? Please read the right column for recommendations.

WITH DEVKIT

Ruby+Devkit 2.6.3-1 (x64)
Ruby+Devkit 2.6.3-1 (x86)
=> **Ruby+Devkit 2.5.5-1 (x64)**
Ruby+Devkit 2.5.5-1 (x86)
Ruby+Devkit 2.4.6-1 (x64)
Ruby+Devkit 2.4.6-1 (x86)

WHICH VERSION TO DOWNLOAD?

If you don't know what version to install and you're getting started with Ruby, we recommend you use **Ruby+Devkit 2.5.X (x64)** installer. It provides the biggest number of compatible gems and installs MSYS2-Devkit alongside Ruby, so that gems with C-extensions can be compiled immediately. The 32 bit (x86) version is recommended only if custom 32 bit native DLLs or COM objects have to be used.

HOW TO UPDATE?

Ruby can be updated to the latest patch version (e.g. from 2.4.1 to 2.4.4)

Figure 23. A-2: Identify Ruby download for your device. Source: [10].

Figure 24 reveal the ruby downloader file to execute on your associated device.

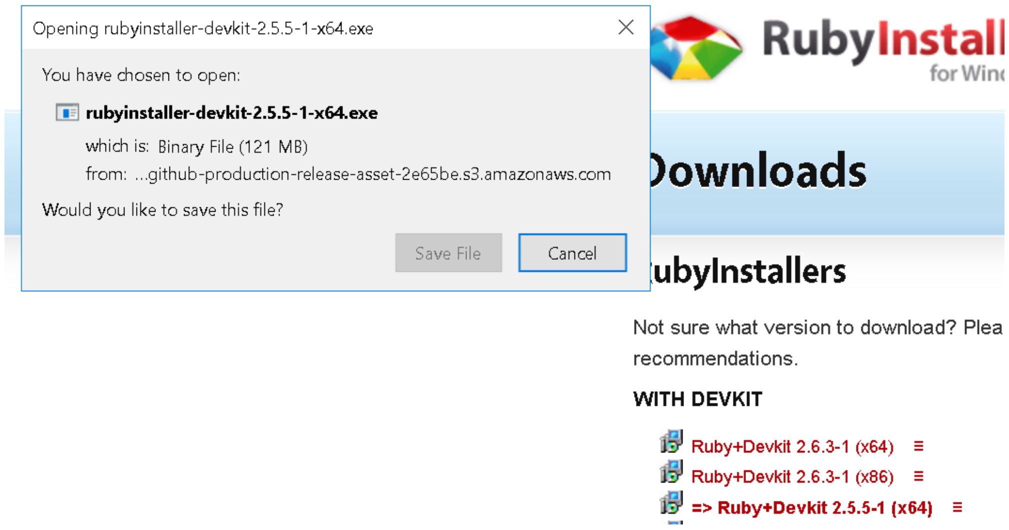
Opening rubyinstaller-devkit-2.5.5-1-x64.exe

You have chosen to open:

rubyinstaller-devkit-2.5.5-1-x64.exe

which is: Binary File (121 MB)

from: ...github-production-release-asset-2e65be.s3.amazonaws.com

Would you like to save this file?

Not sure what version to download? Plea recommendations.

WITH DEVKIT

- Ruby+Devkit 2.6.3-1 (x64)
- Ruby+Devkit 2.6.3-1 (x86)
- => Ruby+Devkit 2.5.5-1 (x64)

Figure 24. A-3: Ruby installer. Source: [10].

Next, after the Ruby installation is confirmed the data farming Ruby scripts must be installed by running the command "**gem install datafarming**," assuming you have a network connection. Figure 25 reveals the commands to execute the stack_nolhs.rb program from Ruby is different between both PC's and Linux machines; however, here I will list the PC commands to make the program execute. Below by typing the command "**stack_nolhs.rb –h**" will list all of the associated commands to execute your desired design space for NOLH.

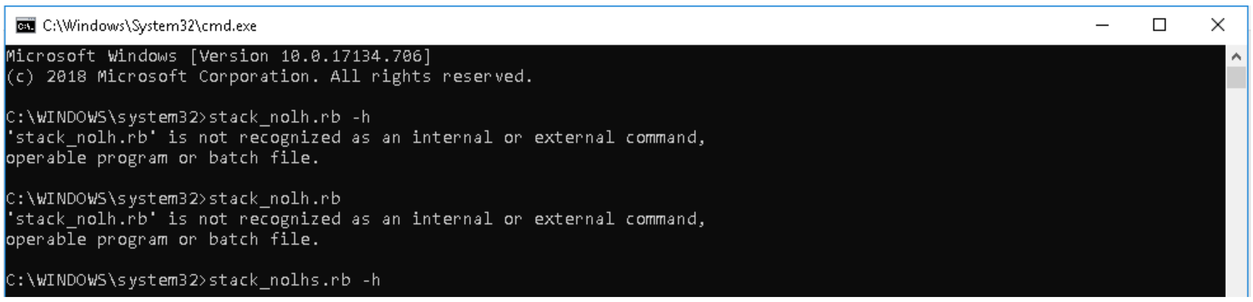
C:\Windows\System32\cmd.exe

```
Microsoft Windows [Version 10.0.17134.706]
(c) 2018 Microsoft Corporation. All rights reserved.

C:\WINDOWS\system32>stack_nolh.rb -h
'stack_nolh.rb' is not recognized as an internal or external command,
operable program or batch file.

C:\WINDOWS\system32>stack_nolh.rb
'stack_nolh.rb' is not recognized as an internal or external command,
operable program or batch file.

C:\WINDOWS\system32>stack_nolhs.rb -h
```

Figure 25. A-4: NOLHS Commands. Source: [10].

Figure 26 reveals the results from calling ruby with the "**-h**" command in the command window.

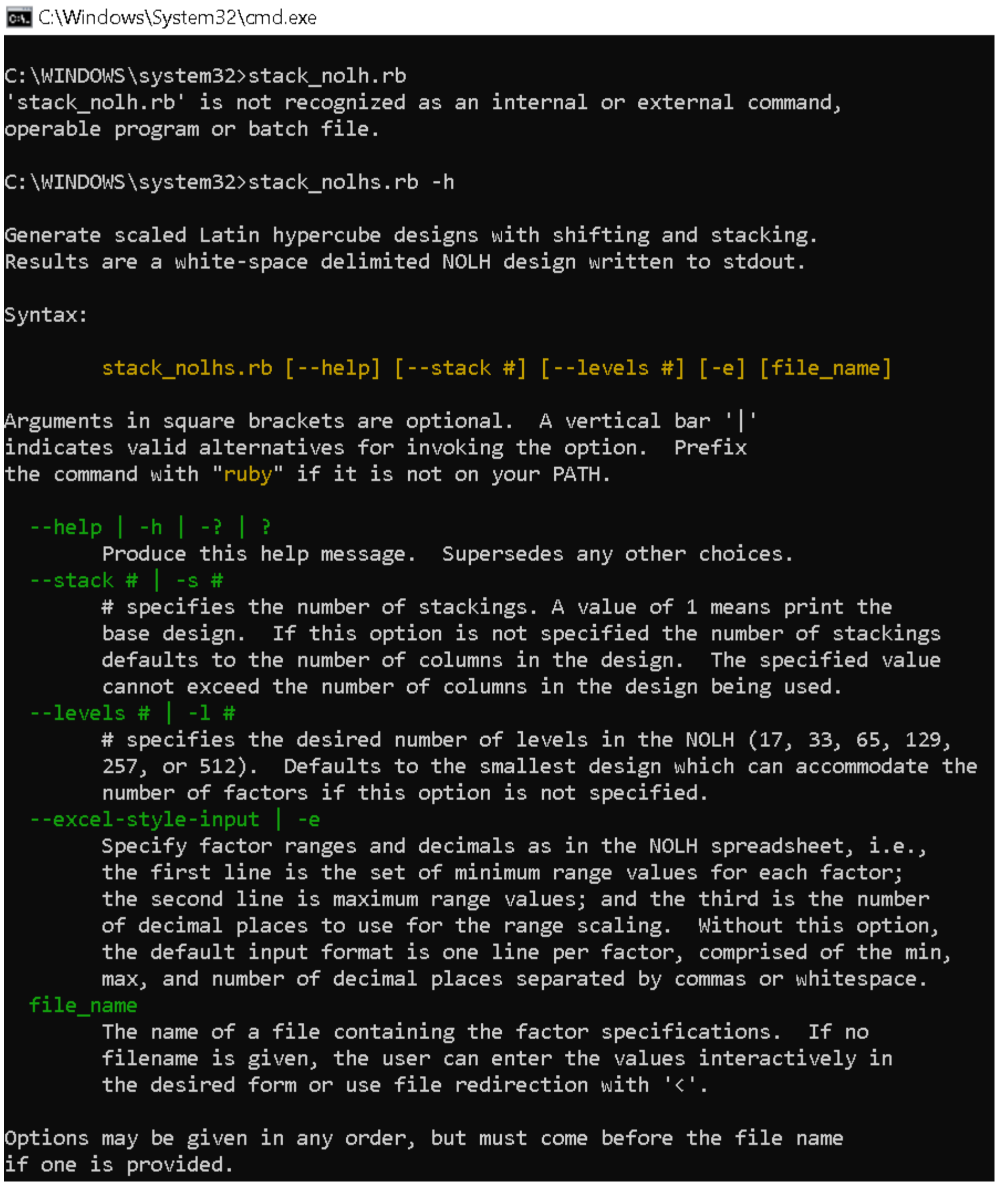

```
C:\Windows\System32\cmd.exe

C:\WINDOWS\system32>stack_nolh.rb
'stack_nolh.rb' is not recognized as an internal or external command,
operable program or batch file.

C:\WINDOWS\system32>stack_nolhs.rb -h

Generate scaled Latin hypercube designs with shifting and stacking.
Results are a white-space delimited NOLH design written to stdout.

Syntax:

        stack_nolhs.rb [--help] [--stack #] [--levels #] [-e] [file_name]

Arguments in square brackets are optional.  A vertical bar '|'
indicates valid alternatives for invoking the option.  Prefix
the command with "ruby" if it is not on your PATH.

  --help | -h | -? | ?
        Produce this help message.  Supersedes any other choices.
  --stack # | -s #
        # specifies the number of stackings. A value of 1 means print the
        base design.  If this option is not specified the number of stackings
        defaults to the number of columns in the design.  The specified value
        cannot exceed the number of columns in the design being used.
  --levels # | -l #
        # specifies the desired number of levels in the NOLH (17, 33, 65, 129,
        257, or 512).  Defaults to the smallest design which can accommodate the
        number of factors if this option is not specified.
  --excel-style-input | -e
        Specify factor ranges and decimals as in the NOLH spreadsheet, i.e.,
        the first line is the set of minimum range values for each factor;
        the second line is maximum range values; and the third is the number
        of decimal places to use for the range scaling.  Without this option,
        the default input format is one line per factor, comprised of the min,
        max, and number of decimal places separated by commas or whitespace.
  file_name
        The name of a file containing the factor specifications.  If no
        filename is given, the user can enter the values interactively in
        the desired form or use file redirection with '<'.

Options may be given in any order, but must come before the file name
if one is provided.
```

Figure 26. A-5: Help Command Results for stack_nolhs.rb. Source: [10].

Next, to familiarize yourself with the results utilized for the research of this research, the following commands were used.

stack_nolhs.rb -s 1 -e <results.txt >mydesign3.csv

The “-s 1” command call the “stack” function to execute “once” for the stack_nolhs.rb program that will return the desired least amount of design points for our design that either returned 129-by-9, without tunnel junctions, or 129-by-11, with tunnel junctions, results for the design.

```
stack_nolhs.rb -l 129 -e <results.txt >mydesign3.csv
```

The “-l 129” commands call the “level” function to execute for “129” levels for the stack_nolhs.rb program that will return the extended amount of design points for our design that either returned 2817-by-9, without tunnel junctions, or 2817-by-11, with tunnel junctions, results for the design.

APPENDIX B. INP PARAMETER FUNCTION

```
function [m_nd,m_ni,eh,el,mp,Egd,Egi]=par_InP
%%This function holds the values and parameters for calculations and
the combined effective mass
%%for use later
m_nd = 0.0795;
m_ni = 0.88;
m_lp = 0.089;
m_hp = 0.6;
eh   = 9.61;
el   = 12.5;
Egd  = 1.4236;
Egi  = 2.273;

mp=(m_lp^1.5+m_hp^1.5)^(2/3);                %Combined effective mass

end
```

THIS PAGE INTENTIONALLY LEFT BLANK

APPENDIX C. GAP PARAMETER FUNCTION

```
function [m_nd,m_ni,eh,el,mp,Egd,Egi]=par_GaP
%%This function holds the values and parameters for calculations and
the combined effective mass
%%for use later
m_nd = 0.13;
m_ni = 1.12;
m_lp = 0.14;
m_hp = 0.79;
eh   = 9.11;
el   = 11.1;
Egd  = 2.87;
Egi  = 2.35;

mp=(m_lp^1.5+m_hp^1.5)^(2/3);    %Combined effective mass
end
```

THIS PAGE INTENTIONALLY LEFT BLANK

APPENDIX D. GAAS PARAMETER FUNCTION

```
function [m_nd,m_ni,eh,el,mp,Egd,Egi]=par_GaAs
%%This function holds the values and parameters for calculations and
the combined effective mass
%%for use later
m_nd = 0.067;
m_ni = 0.85;
m_lp = 0.082;
m_hp = 0.51;
eh   = 10.89;
el   = 13.2;
Egd  = 1.1519;
Egi  = 1.981;

mp=(m_lp^1.5+m_hp^1.5)^(2/3);  %Combined effective mass

end
```

THIS PAGE INTENTIONALLY LEFT BLANK

APPENDIX E. ALAS PARAMETER FUNCTION

```
function [m_nd,m_ni,eh,el,mp,Egd,Egi]=par_AlAs
%%This function holds the values and parameters for calculations and
the combined effective mass
%%for use later
m_nd = 0.15;
m_ni = 0.19;
m_lp = 0.16;
m_hp = 0.81;
eh   = 8.16;
el   = 12;
Egd  = 3.099;
Egi  = 2.24;

mp=(m_lp^1.5+m_hp^1.5)^(2/3); %Combined effective mass

end
```

THIS PAGE INTENTIONALLY LEFT BLANK

APPENDIX F. ALAS MOBILITY FUNCTION

```
function [AlAsmu_n,AlAsmu_p,mu_1n,mu_1p,mu_2n,mu_2p] = mobility_AlAs(T,N)
%This function is used to calculate the mobility of e-'s and h+'s for AlAs

mu_1n=10;
mu_1p=10;

mu_2n=400;
mu_2p=200;

alphan=0;
alphap=0;

betan=-2.1;
betap=-2.24;

gaman=-3;
gamap=-1.464;

sigman=1;
sigmap=.488;

Ncritn=5.46e17;
Ncritp=3.48e17;

%Electron mobility
AlAsmu_n=mu_1n*(T/300)^alphan + (mu_2n*(T/300)^betan - mu_1n*(T/300)^alphan)./(1+(T/300)^gaman.*(N./Ncritn).^sigman);
%Hole mobility
AlAsmu_p=mu_1p*(T/300)^alphap + (mu_2p*(T/300)^betap - mu_1p*(T/300)^alphap)./(1+(T/300)^gamap.*(N./Ncritp).^sigmap);


end
```

THIS PAGE INTENTIONALLY LEFT BLANK

APPENDIX G. GAAS MOBILITY FUNCTION

```
%This function is used to calculate the mobility of e-'s and h+'s for GaAs

function [GaAsmu_n,GaAsmu_p] = mobility_GaAs(T,N)

mu_1n=500;
mu_1p=20;

mu_2n=9400;
mu_2p=491.5;

alphan=0;
alphap=0;

betan=-2.1;
betap=-2.2;

gaman=-1.182;
gamap=-1.14;

sigman=0.394;
sigmap=.38;

Ncritn=6e16;
Ncritp=1.48e17;

%Electron mobility
GaAsmu_n=mu_1n*(T/300)^alphan + (mu_2n*(T/300)^betan - mu_1n*(T/300)^alphan)./(1+(T/300)^gaman.*(N./Ncritn).^sigman);
%Hole mobility
GaAsmu_p=mu_1p*(T/300)^alphap + (mu_2p*(T/300)^betap - mu_1p*(T/300)^alphap)./(1+(T/300)^gamap.*(N./Ncritp).^sigmap);

end
```

THIS PAGE INTENTIONALLY LEFT BLANK

APPENDIX H. GAP MOBILITY FUNCTION

```
%This function is used to calculate the mobility of e-'s and h+'s for GaPh
function [GaPhmu_n,GaPhmu_p,mu_1n,mu_1p,mu_2n,mu_2p] = mobility_GaPh(T,N)

mu_1n=10; mu_1p=10;

mu_2n=152; mu_2p=147;

alphan=0; alphap=0;

betan=-1.6; betap=-1.98;

gaman=-0.568; gamap=0;

sigman=0.8; sigmap=0.85;

Ncritn=4.4e18; Ncritp=1e18;

%Electron mobility
GaPhmu_n=mu_1n*(T/300)^alphan + (mu_2n*(T/300)^betan - mu_1n*(T/300)^alphan)./(1+(T/300)^gaman.*(N./Ncritn).^sigman);
%Hole mobility
GaPhmu_p=mu_1p*(T/300)^alphap + (mu_2p*(T/300)^betap - mu_1p*(T/300)^alphap)./(1+(T/300)^gamap.*(N./Ncritp).^sigmap);

end
```

THIS PAGE INTENTIONALLY LEFT BLANK

APPENDIX I. INP MOBILITY FUNCTION

```
%This function is used to calculate the mobility of e-'s and h+'s for InPh
function [InPhmu_n,InPhmu_p,mu_1n,mu_1p,mu_2n,mu_2p] = mobility_InPh(T,N)

mu_1n=400;
mu_1p=10;

mu_2n=5200;
mu_2p=170;

alphan=0;
alphap=0;

betan=-2;
betap=-2;

gaman=-1.5275;
gamap=-1.86;

sigman=0.47;
sigmap=0.62;

Ncritn=5.46e17;
Ncritp=3.48e17;

%Electron mobility
InPhmu_n=mu_1n*(T/300)^alphan + (mu_2n*(T/300)^betan - mu_1n*(T/300)^alphan)./(1+(T/300)^gaman.*(N./Ncritn).^sigman);
%Hole mobility
InPhmu_p=mu_1p*(T/300)^alphap + (mu_2p*(T/300)^betap - mu_1p*(T/300)^alphap)./(1+(T/300)^gamap.*(N./Ncritp).^sigmap);

end
```

THIS PAGE INTENTIONALLY LEFT BLANK

APPENDIX J.   INGAP WINDOW MOBILITY FUNCTION

```
function [InGaPwmu_n,InGaPwmu_p]=InGaP_window(N)
%%This function takes in the doping concentrations and performs the
%%necessary mobility calculations necessary to input to the associated
%%deckbuild file for Silvaco to run efficiently.

%% Parameters necessary for this function to run effiiciently

T=300;               %Temp set to 300K
k=8.617e-5;          %Plank's constant in eV to be used in conversion later

C=[0.51 0.49];       %Molar fractions/percentages utilized for calculations used late

[m_nd,m_ni,eh,el,mp,Egd,Egi]=par_InP;          %Parameters obtained for InP
eh1=eh;
el1=el;
e1=eh;
e3=el;
m_nd1=m_nd;
m_ni1=m_ni;
mp1=mp;
Eg1=Egd;
Eg11=Egi;

[m_nd,m_ni,eh,el,mp,Egd,Egi]=par_GaP;          %Parameters obtained for GaP
eh2=eh;
el2=el;
e2=eh;
e4=el;
m_nd2=m_nd;
m_ni2=m_ni;
mp2=mp;
Eg2=Egd;
Eg22=Egi;
%% Calculations performed for the following mobilities, while taking into consideration their molar fractional
combinations
[InPhmu_n,InPhmu_p] = mobility_InPh(T,N);       %Mobilities determined for InP
mu_1n=InPhmu_n(5);
[GaPhmu_n,GaPhmu_p] = mobility_GaPh(T,N);       %Mobilities determined for GaP
mu_2n=GaPhmu_n(5);
mu_2p=GaPhmu_p(5);

for i=1:length(C)
    ehh(i)  =(1+2*[C*((e1-1)/(e1+2))+(1-C)*((e2-1)/(e2+2))])/(1-C*((e1-1)/(e1+2))-(1-C)*((e2-1)/(e2+2)));
    ell(i)  =(1+2*[C*((e3-1)/(e3+2))+(1-C)*((e4-1)/(e4+2))])/(1-C*((e3-1)/(e3+2))-(1-C)*((e4-1)/(e4+2)));
    mpp(i)  =(mp2*mp1)/(C(i)*mp2+(1-C(i))*mp1);
    Egd(i)  =(1-C(i))*Eg1+C(i)*Eg2;
    Egi(i)  =(1-C(i))*Eg11+C(i)*Eg22;
end

eh=ehh(1);      %Sets eh
el=ell(2);      %Sets el
Egd=Egd(1);     %Sets the direct bandgap from calculations above
Egi=Egi(1);     %Sets the indirect bandgap from calculations above
mp=mpp(1);      %Sets the combined effective mass from calculations above

mu_d=(mu_2n*m_nd2^1.5*(1/eh2-1/el2))/(m_nd1^1.5*(1/eh-1/el));  %direct mobility
mu_i=(mu_1n*m_ni2^1.5*(1/eh1-1/el1))/(m_ni1^1.5*(1/eh-1/el));  %indirect mobility

Rd=1/(1+(m_ni/m_nd)^1.5*exp((Egd-Egi)/(k*T)));                 %Ratio calculations

InGaPwmu_n=mu_d*Rd+mu_i*(1-Rd);                                %e- mobility for InGaP window
InGaPwmu_p=(mu_2p*mp2^1.5*(1/eh2-1/el2))/(mp^1.5*(1/eh-1/el)); %hole mobility for InGaP window
end
```

THIS PAGE INTENTIONALLY LEFT BLANK

APPENDIX K. INGAP EMITTER MOBILITY FUNCTION

```
function [InGaPemu_n,InGaPemu_p]=InGaP_emitter(N)
%%This function takes in the doping concentrations and performs the
%%necessary mobility calculations necessary to input to the associated
%%deckbuild file for Silvaco to run efficiently.

%% Parameters necessary for this function to run effiiciently

T=300;               %Temp set to 300K
k=8.617e-5;          %Plank's constant in eV to be used in conversion later

C=[0.51 0.49];       %Molar fractions/percentages utilized for calculations used late

[m_nd,m_ni,eh,el,mp,Egd,Egi]=par_InP;          %Parameters obtained for InP
eh1=eh;
el1=el;
e1=eh;
e3=el;
m_nd1=m_nd;
m_ni1=m_ni;
mp1=mp;
Eg1=Egd;
Eg11=Egi;

[m_nd,m_ni,eh,el,mp,Egd,Egi]=par_GaP;          %Parameters obtained for GaP
eh2=eh;
el2=el;
e2=eh;
e4=el;
m_nd2=m_nd;
m_ni2=m_ni;
mp2=mp;
Eg2=Egd;
Eg22=Egi;

%% Calculations performed for the following mobilities, while taking into consideration their molar fractional
combinations
[InPhmu_n,InPhmu_p] = mobility_InPh(T,N);    %Mobilities determined for InP
mu_1n=InPhmu_n(2);
[GaPhmu_n,GaPhmu_p] = mobility_GaPh(T,N);    %Mobilities determined for GaP
mu_2n=GaPhmu_n(2);
mu_2p=GaPhmu_p(2);

for i=1:length(C)
    ehh(i)  =(1+2*[C*((e1-1)/(e1+2))+(1-C)*((e2-1)/(e2+2))])/(1-C*((e1-1)/(e1+2))-(1-C)*((e2-1)/(e2+2)));
    ell(i)  =(1+2*[C*((e3-1)/(e3+2))+(1-C)*((e4-1)/(e4+2))])/(1-C*((e3-1)/(e3+2))-(1-C)*((e4-1)/(e4+2)));
    mpp(i)  =(mp2*mp1)/(C(i)*mp2+(1-C(i))*mp1);
    Egd(i)  =(1-C(i))*Eg1+C(i)*Eg2;
    Egi(i)  =(1-C(i))*Eg11+C(i)*Eg22;
end

eh=ehh(1);  %Sets eh
el=ell(2);  %Sets el
Egd=Egd(1); %Sets the direct bandgap from calculations above
Egi=Egi(1); %Sets the indirect bandgap from calculations above
mp=mpp(1);  %Sets the combined effective mass from calculations above

mu_d=(mu_2n*m_nd2^1.5*(1/eh2-1/el2))/(m_nd1^1.5*(1/eh-1/el)); %direct mobility
mu_i=(mu_1n*m_ni2^1.5*(1/eh1-1/el1))/(m_ni1^1.5*(1/eh-1/el)); %indirect mobility

Rd=1/(1+(m_ni/m_nd)^1.5*exp((Egd-Egi)/(k*T)));                %Ratio calculations

InGaPemu_n=mu_d*Rd+mu_i*(1-Rd);                               %e- mobility for InGaP emitter
InGaPemu_p=(mu_2p*mp2^1.5*(1/eh2-1/el2))/(mp^1.5*(1/eh-1/el));%hole mobility for InGaP emitter
end
```

THIS PAGE INTENTIONALLY LEFT BLANK

APPENDIX L. INGAP BASE MOBILITY FUNCTION

```
function [InGaPbmu_n,InGaPbmu_p]=InGaP_base(N)
%%This function takes in the doping concentrations and performs the
%%necessary mobility calculations necessary to input to the associated
%%deckbuild file for Silvaco to run efficiently.

%% Parameters necessary for this function to run effiiciently

T=300;               %Temp set to 300K
k=8.617e-5;          %Plank's constant in eV to be used in conversion later

C=[0.51 0.49];       %Molar fractions/percentages utilized for calculations used later

[m_nd,m_ni,eh,el,mp,Egd,Egi]=par_InP;          %Parameters obtained for InP
eh1=eh;
el1=el;
e1=eh;
e3=el;
m_nd1=m_nd;
m_ni1=m_ni;
mp1=mp;
Eg1=Egd;
Eg11=Egi;

[m_nd,m_ni,eh,el,mp,Egd,Egi]=par_GaP;          %Parameters obtained for GaP
eh2=eh;
el2=el;
e2=eh;
e4=el;
m_nd2=m_nd;
m_ni2=m_ni;
mp2=mp;
Eg2=Egd;
Eg22=Egi;

%% Calculations performed for the following mobilities, while taking into consideration their molar fractional
combinations
[InPhmu_n,InPhmu_p] = mobility_InPh(T,N);    %Mobilities determined for InP
mu_1n=InPhmu_n(3);
[GaPhmu_n,GaPhmu_p] = mobility_GaPh(T,N);    %Mobilities determined for GaP
mu_2n=GaPhmu_n(3);
mu_2p=GaPhmu_p(3);

for i=1:length(C)
    ehh(i)  =(1+2*[C*((e1-1)/(e1+2))+(1-C)*((e2-1)/(e2+2))])/(1-C*((e1-1)/(e1+2))-(1-C)*((e2-1)/(e2+2)));
    ell(i)  =(1+2*[C*((e3-1)/(e3+2))+(1-C)*((e4-1)/(e4+2))])/(1-C*((e3-1)/(e3+2))-(1-C)*((e4-1)/(e4+2)));
    mpp(i)  =(mp2*mp1)/(C(i)*mp2+(1-C(i))*mp1);
    Egd(i)  =(1-C(i))*Eg1+C(i)*Eg2;
    Egi(i)  =(1-C(i))*Eg11+C(i)*Eg22;
end

eh=ehh(1);             %Sets eh
el=ell(2);             %Sets el
Egd=Egd(1);            %Sets the direct bandgap from calculations above
Egi=Egi(1);            %Sets the indirect bandgap from calculations above
mp=mpp(1);             %Sets the combined effective mass from calculations above


mu_d=(mu_2n*m_nd2^1.5*(1/eh2-1/el2))/(m_nd1^1.5*(1/eh-1/el)); %direct mobility
mu_i=(mu_1n*m_ni2^1.5*(1/eh1-1/el1))/(m_ni1^1.5*(1/eh-1/el)); %indirect mobility

Rd=1/(1+(m_ni/m_nd)^1.5*exp((Egd-Egi)/(k*T)));                %Ratio calculations

InGaPbmu_n=mu_d*Rd+mu_i*(1-Rd);                               %e- mobility for InGaP window
InGaPbmu_p=(mu_2p*mp2^1.5*(1/eh2-1/el2))/(mp^1.5*(1/eh-1/el)); %hole mobility for InGaP window
end
```

THIS PAGE INTENTIONALLY LEFT BLANK

APPENDIX M. INALGAP WINDOW MOBILITY FUNCTION

```
function [InAlGaPwmu_n,InAlGaPwmu_p]=InAlGaP_window(N)
%%This function takes in the doping concentrations and performs the
%%necessary mobility calculations necessary to input to the associated
%%deckbuild file for Silvaco to run efficiently.

%% Parameters necessary for this function to run effiiciently

T=300;               %Temp set to 300K
k=8.617e-5;          %Plank's constant in eV to be used in conversion later

C=[0.53 0.47];%Molar fractions/percentages utilized for calculations used later

[m_nd,m_ni,eh,el,mp,Egd,Egi]=par_AlP;         %Parameters obtained for AlP
eh1=eh;
el1=el;
e1=eh;
e3=el;
m_nd1=m_nd;
m_ni1=m_ni;
mp1=mp;
Eg1=Egd;
Eg11=Egi;

[eh,el,Egd,Egi,mp]=AlGaP_window(N);         %Parameters obtained for AlGaP
eh2=eh;
el2=el;
e2=eh;
e4=el;
m_nd2=m_nd;
m_ni2=m_ni;
mp2=mp;
Eg2=Egd;
Eg22=Egi;

%% Calculations performed for the following mobilities, while taking into consideration their molar fractional
combinations
[GaPhmu_n,GaPhmu_p] = mobility_GaPh(T,N);     %Mobilities determined for GaP
mu_1n=GaPhmu_n(1);
[InPhmu_n,InPhmu_p] = mobility_InPh(T,N);     %Mobilities determined for InP
mu_2n=InPhmu_n(1);
mu_2p=InPhmu_p(1);

for i=1:length(C)
    ehh(i)  =(1+2*[C*((e1-1)/(e1+2))+(1-C)*((e2-1)/(e2+2))]])/(1-C*((e1-1)/(e1+2))-(1-C)*((e2-1)/(e2+2)));
    ell(i)  =(1+2*[C*((e3-1)/(e3+2))+(1-C)*((e4-1)/(e4+2))]])/(1-C*((e3-1)/(e3+2))-(1-C)*((e4-1)/(e4+2)));
    mpp(i)  =(mp2*mp1)/(C(i)*mp2+(1-C(i))*mp1);
    Egd(i)  =(1-C(i))*Eg1+C(i)*Eg2;
    Egi(i)  =(1-C(i))*Eg11+C(i)*Eg22;
end

eh=ehh(1);         %Sets eh
el=ell(2);         %Sets el
Egd=Egd(1);        %Sets the direct bandgap from calculations above
Egi=Egi(1);        %Sets the indirect bandgap from calculations above
mp=mpp(1);         %Sets the combined effective mass from calculations above

mu_d=(mu_2n*m_nd2^1.5*(1/eh2-1/el2))/(m_nd1^1.5*(1/eh-1/el)); %direct mobility
mu_i=(mu_1n*m_ni2^1.5*(1/eh1-1/el1))/(m_ni1^1.5*(1/eh-1/el)); %indirect mobility

Rd=1/(1+(m_ni/m_nd)^1.5*exp((Egd-Egi)/(k*T)));                %Ratio calculations

InAlGaPwmu_n=mu_d*Rd+mu_i*(1-Rd);                                %e- mobility for InAlGaP window
InAlGaPwmu_p=(mu_2p*mp2^1.5*(1/eh2-1/el2))/(mp^1.5*(1/eh-1/el)); %hole mobility for InAlGaP window
end
```

THIS PAGE INTENTIONALLY LEFT BLANK

APPENDIX N.   INALGAP BSF MOBILITY FUNCTION

```
function [InAlGaPbsfmu_n,InAlGaPbsfmu_p]=InAlGaP_bsf(N)
%%This function takes in the doping concentrations and performs the
%%necessary mobility calculations necessary to input to the associated
%%deckbuild file for Silvaco to run efficiently.

%% Parameters necessary for this function to run effiiciently
T=300;                  %Temp set to 300K
k=8.617e-5;             %Plank's constant in eV to be used in conversion later

C=[0.53 0.47];          %Molar fractions/percentages utilized for calculations used later


[m_nd,m_ni,eh,el,mp,Egd,Egi]=par_AlP;  %Parameters obtained for AlP
eh1=eh; el1=el;
e1=eh;
e3=el;
m_nd1=m_nd;
m_ni1=m_ni;
mp1=mp;
Eg1=Egd;
Eg11=Egi;

[eh,el,Egd,Egi,mp]=AlGaP_bsf(N);       %Parameters obtained for AlGaP
eh2=eh;
el2=el;
e2=eh;
e4=el;
m_nd2=m_nd;
m_ni2=m_ni;
mp2=mp;
Eg2=Egd;
Eg22=Egi;

%% Calculations performed for the following mobilities, while taking into consideration their molar fractional
combinations
[GaPhmu_n,GaPhmu_p] = mobility_GaPh(T,N);  %Mobilities determined for GaP
mu_1n=GaPhmu_n(4);
[InPhmu_n,InPhmu_p] = mobility_InPh(T,N);  %Mobilities determined for InP
mu_2n=InPhmu_n(4);
mu_2p=InPhmu_p(4);

for i=1:length(C)
    ehh(i)  =(1+2*[C*((e1-1)/(e1+2))+(1-C)*((e2-1)/(e2+2))])/(1-C*((e1-1)/(e1+2))-(1-C)*((e2-1)/(e2+2)));
    ell(i)  =(1+2*[C*((e3-1)/(e3+2))+(1-C)*((e4-1)/(e4+2))])/(1-C*((e3-1)/(e3+2))-(1-C)*((e4-1)/(e4+2)));
    mpp(i)  =(mp2*mp1)/(C(i)*mp2+(1-C(i))*mp1);
    Egd(i)  =(1-C(i))*Eg1+C(i)*Eg2;
    Egi(i)  =(1-C(i))*Eg11+C(i)*Eg22;
end

eh=ehh(1);           %Sets eh
el=ell(2);           %Sets el
Egd=Egd(1);          %Sets the direct bandgap from calculations above
Egi=Egi(1);          %Sets the indirect bandgap from calculations above
mp=mpp(1);           %Sets the combined effective mass from calculations above

mu_d=(mu_2n*m_nd2^1.5*(1/eh2-1/el2))/(m_nd1^1.5*(1/eh-1/el)); %direct mobility
mu_i=(mu_1n*m_ni2^1.5*(1/eh1-1/el1))/(m_ni1^1.5*(1/eh-1/el)); %indirect mobility

Rd=1/(1+(m_ni/m_nd)^1.5*exp((Egd-Egi)/(k*T)));                %Ratio calculations

InAlGaPbsfmu_n=mu_d*Rd+mu_i*(1-Rd);                                %e- mobility for InAlGaP BSF
InAlGaPbsfmu_p=(mu_2p*mp2^1.5*(1/eh2-1/el2))/(mp^1.5*(1/eh-1/el)); %hole mobility for InAlGaP BSF
end
```

THIS PAGE INTENTIONALLY LEFT BLANK

APPENDIX O. ALGAP WINDOW PARAMETER FUNCTION

```
function [eh,el,Egd,Egi,mp]=AlGaP_window(N)

T=300;
k=8.617e-5;

C=[0.7 0.3];

[m_nd,m_ni,eh,el,mp,Egd,Egi]=par_AlP;
eh1=eh;
el1=el;
e1=eh;
e3=el;
m_nd1=m_nd;
m_ni1=m_ni;
mp1=mp;
Eg1=Egd;
Eg11=Egi;

[m_nd,m_ni,eh,el,mp,Egd,Egi]=par_GaP;
eh2=eh;
el2=el;
e2=eh;
e4=el;
m_nd2=m_nd;
m_ni2=m_ni;
mp2=mp;
Eg2=Egd;
Eg22=Egi;

[GaPhmu_n,GaPhmu_p] = mobility_GaPh(T,N);
mu_1n=GaPhmu_n(:,1);
[InPhmu_n,InPhmu_p] = mobility_InPh(T,N);
mu_2n=InPhmu_n(:,1);
mu_2p=InPhmu_p(:,1);

for i=1:length(C)
    ehh(i)  =(1+2*[C*((e1-1)/(e1+2))+(1-C)*((e2-1)/(e2+2))])/(1-C*((e1-1)/(e1+2))-(1-C)*((e2-1)/(e2+2)));
    ell(i)  =(1+2*[C*((e3-1)/(e3+2))+(1-C)*((e4-1)/(e4+2))])/(1-C*((e3-1)/(e3+2))-(1-C)*((e4-1)/(e4+2)));
    mpp(i)  =(mp2*mp1)/(C(i)*mp2+(1-C(i))*mp1);
    Egd(i)  =(1-C(i))*Eg1+C(i)*Eg2;
    Egi(i)  =(1-C(i))*Eg11+C(i)*Eg22;
end

eh=ehh(1);
el=ell(2);
Egd=Egd(1);
Egi=Egi(1);
mp=mpp(1);

end
```

THIS PAGE INTENTIONALLY LEFT BLANK

APPENDIX P. ALGAAS MOBILITY FUNCTION

```
function [AlGaAsbsfmu_n,AlGaAsbsfmu_p]=AlGaAs_bsf(N)
% clear all; clc;

% [N,design_thickness]=input_decks(1,0,1,1,1);

T=300;
k=8.617e-5;

C=[0.7 0.3];

[m_nd,m_ni,eh,el,mp,Egd,Egi]=par_AlAs;
eh1=eh;
el1=el;
e1=eh;
e3=el;
m_nd1=m_nd;
m_ni1=m_ni;
mp1=mp;
Eg1=Egd;
Eg11=Egi;

[m_nd,m_ni,eh,el,mp,Egd,Egi]=par_GaAs;
eh2=eh;
el2=el;
e2=eh;
e4=el;
m_nd2=m_nd;
m_ni2=m_ni;
mp2=mp;
Eg2=Egd;
Eg22=Egi;

[AlAsmu_n,AlAsmu_p] = mobility_AlAs(T,N);
mu_1n=AlAsmu_n(8);
[GaAsmu_n,GaAsmu_p] = mobility_GaAs(T,N);
mu_2n=GaAsmu_n(8);
mu_2p=GaAsmu_p(8);

for i=1:length(C)
    ehh(i)  =(1+2*[C*((e1-1)/(e1+2))+(1-C)*((e2-1)/(e2+2))])/(1-C*((e1-1)/(e1+2))-(1-C)*((e2-1)/(e2+2)));
    ell(i)  =(1+2*[C*((e3-1)/(e3+2))+(1-C)*((e4-1)/(e4+2))])/(1-C*((e3-1)/(e3+2))-(1-C)*((e4-1)/(e4+2)));
    mpp(i)  =(mp2*mp1)/(C(i)*mp2+(1-C(i))*mp1);
    Egd(i)  =(1-C(i))*Eg1+C(i)*Eg2;
    Egi(i)  =(1-C(i))*Eg11+C(i)*Eg22;
end

eh=ehh(1);
el=ell(2);
Egd=Egd(1);
Egi=Egi(1);
mp=mpp(1);

mu_d=(mu_2n*m_nd2^1.5*(1/eh2-1/el2))/(m_nd1^1.5*(1/eh-1/el));
mu_i=(mu_1n*m_ni2^1.5*(1/eh1-1/el1))/(m_ni1^1.5*(1/eh-1/el));

Rd=1/(1+(m_ni/m_nd)^1.5*exp((Egd-Egi)/(k*T)));

AlGaAsbsfmu_n=mu_d*Rd+mu_i*(1-Rd);
AlGaAsbsfmu_p=(mu_2p*mp2^1.5*(1/eh2-1/el2))/(mp^1.5*(1/eh-1/el));
end
```

THIS PAGE INTENTIONALLY LEFT BLANK

APPENDIX Q. CREATE DESIGN SPACE VECTOR

```
function [N,design_thickness]=input_decks(TJ,on_off,linux_PC,ruby,model)
%
%      [N,design_thickness]=input_decks(TJ,on_off,linux_PC,ruby,model)
%
% This function calls get_designspace with the following inputs
% TJ=0, runs the get_designspace with only 18 factors
% TJ=1, runs the get_designspace with 22 factors including the tunnel
% junction thicknesses
%
% on_off=1, provides command to plot the resulting mobilities from either
% TJ=0/1 results
% on_off=0, provides command not to plot the resulting mobilities from
% either TJ=0/1 results
%
%  **Note: Linux execution will only work if the user opens Matlab in the**
%  **Public folder, due to that's the current location of the Ruby25x-64***
%  **library.**************************************************************
%
% linux_PC=1, performs command line for PC execution
% linux_PC=0, performs command line for linux execution
%
% ruby=1, runs the stack command that provides 129 design points for 18-22
% factors
% ruby=0, runs the level command that provides 2817 design points for 18-22
% factors
%
% model=0, runs the thicknesses and doping concentratons for for 18-22
% factors derived from the original model
% model=1, runs the thicknesses and doping concentratons (including TJ's)
% from the original model

base=0.55; %orginal base thickness
perc=.50;  %percentage difference
% bmin=base - base*perc;
% bmax=base + base*perc;
bmin=0.53;
bmax=0.57;

if TJ==0
factors=18;
t_min = [0.01 0.02 bmin 0.01 0.02 0.48 2.03 0.08 0.18];
t_max = [0.05 0.06 bmax 0.05 0.06 0.52 2.07 0.12 0.22];
N_min = [17   17    15    17     17    17    16     17    17];
N_max = [19   19    17    19     19    19    18     19    19];
else
factors=22;
t_min = [0.01 0.02 bmin 0.01 0.02 0.48 2.03 0.08 0.18 0.005 0.005];
t_max = [0.05 0.06 bmax 0.05 0.06 0.52 2.07 0.12 0.22 0.045 0.045];
N_min = [17   17    15    17    17    17    16    17    17   18   18];
N_max = [19   19    17    19    19    19    18    19    19   20   20];
end


[N,design_thickness]=get_designspace(factors,t_min,t_max,N_min,N_max,on_off,linux_PC,ruby,model);
```

THIS PAGE INTENTIONALLY LEFT BLANK

APPENDIX R. CREATE DESIGN SPACE FROM RUBY

```
function [N,design_thickness]=get_designspace(factors,t_min,t_max,N_min,N_max,on_off,linux_PC,ruby,model)
%
% [N,design_thickness]=get_designspace(factors,t_min,t_max,N_min,N_max,on_off,linux_PC,ruby,model)
%
% Creates the needed .txt file for the desired inputs for NOLH to run and
% returns N (doping concentration) and thicknesses (design_thickness) for
% use in Silvaco
%
% factors should be entered in as a factor of 2, due to this function will
% always need an input for thickness and doping concetrations for each
% experimental run, factors should be atleast 2, but this can perform up to 22 factors
%
% t_min and t_max are inputs for min and max thicknesses expected in microns
%
% N_min and N_max are inputs for min and max doping concentrations interms
%                 of the exponent desired
%
% on_off=1, performs mobility check,
% on_off=0, turns off mobility check
%
%  **Note: Linux execution will only work if the user opens Matlab in the**
%  **Public folder, due to that's the current location of the Ruby25x-64***
%  **library.*************************************************************
%
% linux_PC=1, performs command line for PC execution
% linux_PC=0, performs command line for linux execution
%
% ruby=1, runs the stack command that provides 129 design points for 18-22
%         factors
% ruby=0, runs the level command that provides 2817 design points for 18-22
%         factors
%
% model=0, runs the thicknesses and doping concentratons for for 18-22
%          factors derived from the original model
% model=1, runs the thicknesses and doping concentratons (including TJ's)
%          from the original model, bypasses NOLH completely

if model==0 %Calls for NOLH to execute

%% Number of factors that're being computed
x1_txt = factors;

%% Min and Max of thicknesses entered

size2  = x1_txt/2;         %1/2's the factor for allocation of the thickness array
x2_txt = zeros(size2,1);   %creates the array for thickness based on allocation from factors
x2_txt = t_min;            %takes input from min thickness for use below

size22  = x1_txt/2;        %1/2's the factor for allocation of the thickness array
x22_txt = zeros(size22,1); %creates the array for thickness based on allocation from factors
x22_txt = t_max;           %takes input from max thickness for use below

%% Max and Min of doping concentrations entered

size3  = x1_txt/2;         %1/2's the factor for allocation of the doping concentration array
x3_txt = zeros(size3,1);   %creates the array for doping concentration based on allocation from factors
x3_txt = N_min;            %takes input from min doping concentration for use below

size33  = x1_txt/2;        %1/2's the factor for allocation of the doping concentration array
x33_txt = zeros(size3,1);  %creates the array for doping concentration based on allocation from factors
x33_txt = N_max;           %takes input from max doping concentration for use below

%% Combine the results for the min and max entered for assimilation below

LB_thick=zeros(size2,1);   %Creates the allocation for the lower bounds for thickness
UB_thick=zeros(size2,1);   %Creates the allocation for the upper bounds for thickness

LB_dop=zeros(size2,1);     %Creates the allocation for the lower bounds for doping concentration
UB_dop=zeros(size2,1);     %Creates the allocation for the upper bounds for doping concentration

dec=zeros(size2,1);        %Creates the allocation for the decimal places input needed for Ruby

sizeA=x1_txt;              %Creates the value needed for the length of the associated for loops below

for i=1:sizeA/2
    LB_thick(i)=x2_txt(i);  %Fills the lower bounds of thickness
    UB_thick(i)=x22_txt(i); %Fills the upper bounds of thickness
    LB_dop(i)=x3_txt(i);    %Fills the lower bounds of doping concentrations
    UB_dop(i)=x33_txt(i);   %Fills the upper bounds of doping concentrations
end

for i=1:sizeA
    dec(i)=3;               %Fills the needed decimal places input for Ruby based on all input factors
end

fid = fopen('results.txt', 'wt' );  %Opens/creates the .txt file for fill in below
```

```
for i=1:length(LB_thick)
   fprintf(fid,"%1d %1d",LB_thick(i),LB_dop(i)); %Fills/prints the min thickness and doping concentrations respectively
   fprintf(fid," ");
end

fprintf(fid,"\n");                               %Ensures next line

for i=1:length(UB_thick)
   fprintf(fid,"%1d %1d",UB_thick(i),UB_dop(i)); %Fills/prints the max thickness and doping concentrations respectively
   fprintf(fid," ");
end

fprintf(fid,"\n");                               %Ensures next line

for i=1:length(dec)
   fprintf(fid,"%1d",dec(i));                    %Fills/prints the decimal input
   fprintf(fid," ");
end

fprintf(fid,"\n");                               %Ensures next line

fclose(fid);                                     %Closes the .txt file

%% Execution of Ruby and NOLHS

% if linux_PC==0
%     if ruby==1
%         command = '/usr/local/bin/ruby stack_nolhs.rb -s 1 -e <results.txt >mydesign3.csv ';
%     else
%         command = '/usr/local/bin/ruby stack_nolhs.rb -l 129 -e <results.txt >mydesign3.csv ';
%     end
% else
if linux_PC==0
    if ruby==1
        command = 'stack_nolhs.rb -s 1 -e <results.txt >mydesign3.csv ';
    elseif ruby==2
        command = 'stack_nolhs.rb -s 2 -e <results.txt >mydesign3.csv ';
    elseif ruby==3
        command = 'stack_nolhs.rb -s 3 -e <results.txt >mydesign3.csv ';
    elseif ruby==4
        command = 'stack_nolhs.rb -s 4 -e <results.txt >mydesign3.csv ';
    elseif ruby==5
        command = 'stack_nolhs.rb -s 5 -e <results.txt >mydesign3.csv ';
    elseif ruby==6
        command = 'stack_nolhs.rb -l 129 -e <results.txt >mydesign3.csv ';
    end
else
    if ruby==1
        command ='CMD /C stack_nolhs.rb -s 1 -e <results.txt >mydesign3.csv ';  %Calls the ruby program and uses the
.txt file just created
    else
        command ='CMD /C stack_nolhs.rb -l 129 -e <results.txt >mydesign3.csv ';
    end
end

status=system(command);                                              %actually calls the command implemented above


design=Table2array(readTable('mydesign3.csv'));                      %converts .csv data into readable data for
Matlab

%% Create individual matrices of resulting NOLH data for thicknesses and doping concentrations

rows=length(design(:,1));                                     %creates the needed length of rows for the design
array
columns=length(design(1,:));                                  %creates the needed length of columns for the design
array
thickness=zeros(rows,columns/2);                              %creates thickness array for data
for i=1:length(columns/2)
    thickness(:,1:end)=design(:,1:2:end);                     %fills every other element of design array
end                                                           %receives every odd column

doping=zeros(rows,columns/2);                                 %creates doping array for data
for i=1:length(columns/2)
    doping(:,1:end)=design(:,2:2:end);                         %fills every other element of design array
end                                                            %receives every odd column
else                                  %cancels NOLH to use the model parameters below with the
                                      %TJ thicknesses and doping concentrations

doping    = [18   18  16  18  18 18   17 18 18   19   19]; %original model doping concentrations
thickness = [.03 .05 .55 .03 .04 .5 2.05 .1 .2 .025 .025]; %original model thicknesses
end
%% Call mobility functions and utilize the doping concebtrations derived from ruby
power=10.^doping;                  %converts doping data into the form needed for our Silvaco
N=power;
design_thickness=thickness;
if on_off==1
     mob_test(N)                                 %checks results of doping concentrations with mobility plots
else                                             %turns on/off mobility check of doping concentrations
end
```

APPENDIX S. CREATE DATA VECTORS FROM .LOG FILE

```
function [eff,Voc, Jsc, FF]=get_designEff(N)
% This function retrieves the efficiencies,open circuit voltage, and  short
% circuit current of the all designs created and places them into an
% usuable array

% [N,design_thickness]=input_decks(1,0,0,1,0);

eff=[];     %creates array for efficency
Voc=[];     %creates array for open circuit voltage
Jsc=[];     %creates array for short circuit current
FF =[];     %creates array for Fill Factor

for j=1:length(N(:,1))
        command=sprintf('forward_IVSimpleTJ%d.log',j);    %generates usable command for a .log file
command to be scripted
%         command=command;
        if isfile(command)                                %checks to see whether or not .log file
exists
           [emitterV,emitterVV,baseC,baseCC]=emitter_baseRead(command); %performs execution to pull
and read data for current and voltage values from the .log file
%                disp(j)
%                disp(solarCell_eff(emitterV,emitterVV,baseC,baseCC));
           [effout, Vocout, Jscout, FFout] = solarCell_eff(emitterV,emitterVV,baseC,baseCC);
%performs desired calculations for the efficiency for each design
           [eff]=[eff effout];                           %creates array for efficiency
           [Voc]=[Voc Vocout];                           %creates array for open circuit voltage
           [Jsc]=[Jsc Jscout];                           %creates array for short circuit current
           [FF] =[FF FFout];                             %creates array for Fill Factor
        else
           eff=[eff 0];  %ensures efficiency array is filled even though .log file may have errorneous
data
           Voc=[Voc 0];  %ensures open circuit voltage array is filled even though .log file may have
errorneous data
           Jsc=[Jsc 0];  %ensures short circuit current array is filled even though .log file may have
errorneous data
           FF =[FF  0];  %ensures Fill Factor array is filled even though .log file may have
errorneous data
        end
    end

end
```

THIS PAGE INTENTIONALLY LEFT BLANK

APPENDIX T. READ DATA FROM .LOG FILE

```
function [emitterV,emitterVV,baseC,baseCC]=emitter_baseRead(command)
%% This function reads .log files produced from Silvaco ATLAS

s = dir(command);

if(s.bytes>0)

    testlogfile = fopen(command); %loads .log file from Silvac

    emitterV = [];                          %creates array for Emitter Voltage
for plotting
    baseC = [];                             %creates array for Base Current for
plotting

    emitterVV = [];                         %creates array for Emitter Voltage
for calculations
    baseCC = [];                            %creates array for Base Current for
calculations

    tline = fgetl(testlogfile);            %reads line from file and discards
newline character
    while ischar(tline)                    %checks if input is a character
array
        datavals = strsplit(tline);        %splts string at the delimiter
        if(datavals{1}=='d')               %checks for character 'd' to start
reading from .log file
            if (str2num(datavals{21})>0)
            emitterV  = [emitterV str2num(datavals{13})];  %{14} fills array
for Emitter Voltage values
            baseC     = [baseC    str2num(datavals{21})];  %{18} fills array
for Base Current values
            end
            emitterVV  = [emitterVV str2num(datavals{13})];  %{14} fills array
for Emitter Voltage values
            baseCC     = [baseCC    str2num(datavals{21})];  %{18}fills array
for Base Current values
        end
        tline = fgetl(testlogfile);        %ensures lines from .log file are
read and discards newline character
    end

    fclose(testlogfile);                   %closes .log file from Silvaco

else
    emitterV = [0];
    baseC = [1];
    emitterVV = [0];
    baseCC = [1];
end
```

THIS PAGE INTENTIONALLY LEFT BLANK

APPENDIX U. CREATE $\eta, V_{OC}, J_{SC}, \& FF$ FROM .LOG FILE

```
function [eff,Voc,Jsc,FF]=solarCell_eff(emitterV,emitterVV,baseC,baseCC)
%% Calculating further parameters necessary for calculations for the
performance of our solar cell
%Constants needed
q=1.61e-19;                 %charge of one electron
kT_q=0.0259;                %Einsten relationship
Pin=135;                    %Input power efficiency at AM0 in mW/cm^2
% Pin=100;                  %Input power efficiency at AM1.5 in mW/cm^2
factor=1e11;

%Calculations for the short circuit current
Jsc=baseC(1)*factor;        %Calculates the short circuit current density in
mA/cm^2

%Finding the point where the current is approximately zero
loc_neg = find(baseCC<0,1);              %locates first negative value
loc_pos = find(baseCC>0,length(baseCC)); %locates positive values

if(~isempty(loc_neg))                        %checks whether loc_neg is emtpy
    last_pos=loc_pos(end);                   %locates last positive value
    y1=baseCC(loc_neg)*factor;               %provides the negative value of
the current
    y2=baseCC(last_pos)*factor;              %provides the last positive value
of the current
    dy=y2-y1;                                %change in y
    x1=emitterVV(loc_neg);                   %provides the value of voltage
respective to current
    x2=emitterVV(last_pos);                  %provides the value of voltage
respective to current
    dx=x2-x1;                                %change in x
    m=dy/dx;                                 %calculates slope, m
    b=y1-m*x1;                               %calculates constant for slope
intercept equation
    Voc=-y1/m+x1;                    %calculates Voc for the design

    FF=trapz(emitterV,baseC.*factor)/(Jsc*Voc);  %Calculates the Fill Factor of
the Solar Cell
    Pout=Jsc*Voc*FF;    %Calculates the output power of the solar cell
    eff=Pout/Pin;                                %Calculates the efficiency of
the solar cell
else                                         %if loc_neg is empty a zero is
applied to the following
    Voc=0;
    FF=0;
    Pout=0;
    eff=0;
end
end
```

THIS PAGE INTENTIONALLY LEFT BLANK

APPENDIX V. CREATING DECKBUILD FILES

```matlab
function creating_inputSimpleTJDecks(N,design_thickness)
%% The purpose of this function is to create deckbuild files for pre-defined design space.

design_thickness=design_thickness;

[InAlGaPwmu_n,InAlGaPwmu_p]     = InAlGaP_window(N);
[InGaPemu_n,InGaPemu_p]         = InGaP_emitter(N);
[InGaPbmu_n,InGaPbmu_p]         = InGaP_base(N);
[InAlGaPbsfmu_n,InAlGaPbsfmu_p] = InAlGaP_bsf(N);

[GaAsTJnmu_n,GaAsTJnmu_p,GaAsTJpmu_n,GaAsTJpmu_p,GaAsenmu_n,GaAsenmu_p,GaAsbnmu_n,GaAsbnmu_p,GaAsbufnmu_n,GaAsbufnmu_p]=GaAs(N);

[InGaPwmu_n,InGaPwmu_p]         = InGaP_window(N);
[AlGaAsbsfmu_n,AlGaAsbsfmu_p]   = AlGaAs_bsf(N);


for i=1:length(N(:,1))

tp_window  =design_thickness(i,1); %replacing line 4
tp_emitter =design_thickness(i,2); %replacing line 5
tp_base    =design_thickness(i,3); %replacing line 6
tp_BSF     =design_thickness(i,4); %replacing line 7

windowp_d  =N(i,1);                %replacing line 10
emitterp_d =N(i,2);                %replacing line 11
basep_d    =N(i,3);                %replacing line 12
BSFp_d     =N(i,4);                %replacing line 13

tp_TJ      =design_thickness(i,10); %replacing line 22
TJ_d       =N(i,10);                %replacing line 23

tb_window  =design_thickness(i,5); %replacing line 34
tb_emitter =design_thickness(i,6); %replacing line 35
tb_base    =design_thickness(i,7); %replacing line 36
tb_BSF     =design_thickness(i,8); %replacing line 37
tb_buffer  =design_thickness(i,9);

windowb_d  =N(i,5);                %replacing line 39
emitterb_d =N(i,6);                %replacing line 40
baseb_d    =N(i,7);                %replacing line 41
BSFb_d     =N(i,8);                %replacing line 42
bufferb_d  =N(i,9);

% fileID = fopen('test5_%dTJ.in','w',i);
fileID = fopen(sprintf('test6_%dTJ.in',i),'w');

fprintf(fileID,'go ATLAS simflags = "-P 2"\n\n');

fprintf(fileID,'#solar top section cell thicknesses set\n');
fprintf(fileID,'set tp_window  =');
fprintf(fileID,'%6.2f\n',tp_window);

fprintf(fileID,'set tp_emitter =');
fprintf(fileID,'%6.2f\n',tp_emitter);

fprintf(fileID,'set tp_base    =');
fprintf(fileID,'%6.2f\n',tp_base)

fprintf(fileID,'set tp_BSF     =');
fprintf(fileID,'%6.2f\n\n',tp_BSF);

fprintf(fileID,'#solar top section cell doping concentrations set\n');
fprintf(fileID,'set windowp_d  =');
fprintf(fileID,'%6.2g\n',windowp_d);

fprintf(fileID,'set emitterp_d =');
fprintf(fileID,'%6.2g\n',emitterp_d);

fprintf(fileID,'set basep_d    =');
fprintf(fileID,'%6.2g\n',basep_d);

fprintf(fileID,'set BSFp_d     =');
fprintf(fileID,'%6.2g\n\n',BSFp_d);

fprintf(fileID,'#Top section mole compositions & affinity settings\n');
fprintf(fileID,'set wp_comp    = 0.49\n');
fprintf(fileID,'set bsfp_comp  = 0.7\n');
fprintf(fileID,'set InGaP_aff  = 3.87\n');
fprintf(fileID,'set AlGaAs_aff = 3.81\n\n');

fprintf(fileID,'#solar cell TJ \n');
fprintf(fileID,'set tp_TJ      = 0.025\n');
% fprintf(fileID,'%6.2d\n',0.025);
fprintf(fileID,'set TJ_d       = 5e19\n\n');
% fprintf(fileID,'%6.2g\n\n',5e19);
```

```
fprintf(fileID,'set p_window   = $tp_window\n');
fprintf(fileID,'set p_emitter  = $p_window+$tp_emitter\n');
fprintf(fileID,'set p_base     = $p_emitter+$tp_base\n');
fprintf(fileID,'set p_bsf      = $p_base+$tp_BSF\n\n');

fprintf(fileID,'set p_TJ       = $p_BSF+$tp_TJ\n');
fprintf(fileID,'set n_TJ       = $p_TJ+$tp_TJ\n\n');

fprintf(fileID,'#solar bottom section cell thicknesses set\n');
fprintf(fileID,'set tb_window  =');
fprintf(fileID,'%6.2f\n',tb_window);

fprintf(fileID,'set tb_emitter =');
fprintf(fileID,'%6.2f\n',tb_emitter);

fprintf(fileID,'set tb_base    =');
fprintf(fileID,'%6.2f\n',tb_base);

fprintf(fileID,'set tb_BSF     =');
fprintf(fileID,'%6.2f\n',tb_BSF);

fprintf(fileID,'set tb_buffer  =');
fprintf(fileID,'%6.2f\n\n',tb_buffer);

fprintf(fileID,'#solar bottom section cell doping concentrations set\n');
fprintf(fileID,'set windowb_d  =');
fprintf(fileID,'%6.2g\n',windowb_d);

fprintf(fileID,'set emitterb_d =');
fprintf(fileID,'%6.2g\n',emitterb_d);

fprintf(fileID,'set baseb_d    =');
fprintf(fileID,'%6.2g\n',baseb_d);

fprintf(fileID,'set BSFb_d     =');
fprintf(fileID,'%6.2g\n',BSFb_d);

fprintf(fileID,'set bufferb_d  =');
fprintf(fileID,'%6.2g\n\n',bufferb_d);

fprintf(fileID,'#Bottom section mole compositions & affinity settings\n');
fprintf(fileID,'set wb_comp    = 0.49\n');
fprintf(fileID,'set bsfb_comp  = 0.7\n\n');

fprintf(fileID,'set b_window   = $n_TJ+$tb_window\n');
fprintf(fileID,'set b_emitter  = $b_window+$tb_emitter\n');
fprintf(fileID,'set b_base     = $b_emitter+$tb_base\n');
fprintf(fileID,'set b_bsf      = $b_base+$tb_BSF\n');
fprintf(fileID,'set b_buffer   = $b_bsf+$tb_buffer\n\n');

fprintf(fileID,'mesh\n');
fprintf(fileID,'x.mesh location=0               spacing=1 \n');
fprintf(fileID,'x.mesh location=1               spacing=1\n');
fprintf(fileID,'y.mesh location=0               spacing=$tp_window/20\n');
fprintf(fileID,'y.mesh location=$p_window       spacing=$tp_window/20\n');
fprintf(fileID,'y.mesh location=$p_emitter      spacing=$tp_emitter/100\n');
fprintf(fileID,'y.mesh location=$p_base         spacing=$tp_base/5\n');
fprintf(fileID,'y.mesh location=$p_bsf          spacing=$tp_BSF/100\n\n');

fprintf(fileID,'y.mesh location=$p_TJ           spacing=$tp_TJ/40\n');
fprintf(fileID,'#y.mesh location=$p_TJ+$tp_TJ    spacing=$tp_TJ/120\n');
fprintf(fileID,'y.mesh location=$n_TJ           spacing=$tp_TJ/40\n\n');

fprintf(fileID,'y.mesh location=$b_window       spacing=$tb_window/20\n');
fprintf(fileID,'y.mesh location=$b_emitter      spacing=$tb_emitter/100\n');
fprintf(fileID,'y.mesh location=$b_base         spacing=$tb_base/5\n');
fprintf(fileID,'y.mesh location=$b_bsf          spacing=$tb_BSF/100\n');
fprintf(fileID,'y.mesh location=$b_buffer       spacing=$tb_buffer/100\n\n');

fprintf(fileID,'#Top Section\n');
fprintf(fileID,'region num=1 material=InAlGaP x.min=0 y.min=0 x.max=1    y.max=$p_window   x.comp = 0.371 y.comp =
0.159\n');
fprintf(fileID,'region num=2 material=InGaP   x.min=0 y.min=$p_window    y.max=$p_emitter  x.comp=0.49 \n');
fprintf(fileID,'region num=3 material=InGaP   x.min=0 y.min=$p_emitter   y.max=$p_base     x.comp=0.49\n');
fprintf(fileID,'region num=4 material=InAlGaP x.min=0 y.min=$p_base      y.max=$p_bsf      x.comp = 0.371 y.comp =
0.159\n\n');

fprintf(fileID,'#tunnel junction\n');
fprintf(fileID,'region num=5 material=GaAs x.min=0 x.max=1 y.min=$p_bsf y.max=$p_TJ\n');
fprintf(fileID,'region num=6 material=GaAs x.min=0 x.max=1 y.min=$p_TJ  y.max=$n_TJ\n\n');

fprintf(fileID,'#Bottom Section\n');
fprintf(fileID,'region num=7  material=InGaP  x.min=0  y.min=$n_TJ       y.max=$b_window x.comp=0.49\n');
fprintf(fileID,'region num=8  material=GaAs   x.min=0  y.min=$b_window   y.max=$b_emitter\n');
fprintf(fileID,'region num=9  material=GaAs   x.min=0  y.min=$b_emitter  y.max=$b_base \n');
fprintf(fileID,'region num=10 material=AlGaAs x.min=0  y.min=$b_base     y.max=$b_bsf    x.comp=0.7\n');
fprintf(fileID,'region num=11 material=GaAs   x.min=0  y.min=$b_bsf      y.max=$b_buffer\n\n');

fprintf(fileID,'electrode name=Emitter  top\n');
fprintf(fileID,'electrode name=tunnel   x.min=0 x.max=1 y.min=$p_bsf y.max=$n_TJ material=GaAs\n');
fprintf(fileID,'electrode name=Base     bottom \n\n');

fprintf(fileID,'#For the top section\n');
fprintf(fileID,'doping p.type uniform concentration=$windowp_d   y.min=0              y.max=$p_window\n');
fprintf(fileID,'doping p.type uniform concentration=$emitterp_d  y.min=$p_window      y.max=$p_emitter\n');
fprintf(fileID,'doping n.type uniform concentration=$basep_d     y.min=$p_emitter     y.max=$p_base\n');
fprintf(fileID,'doping n.type uniform concentration=$BSFp_d      y.min=$p_base        y.max=$p_bsf\n\n');

fprintf(fileID,'#For the bottom section\n');
% fprintf(fileID,'doping p.type uniform concentration=$windowb_d   y.min=$n_TJ          y.max=$b_window\n');
fprintf(fileID,'doping p.type uniform concentration=$windowb_d   y.min=$p_bsf         y.max=$b_window\n');
fprintf(fileID,'doping p.type uniform concentration=$emitterb_d  y.min=$b_window      y.max=$b_emitter\n');
fprintf(fileID,'doping n.type uniform concentration=$baseb_d     y.min=$b_emitter     y.max=$b_base\n');
fprintf(fileID,'doping n.type uniform concentration=$BSFb_d      y.min=$b_base        y.max=$b_bsf\n');
fprintf(fileID,'doping n.type uniform concentration=$bufferb_d   y.min=$b_bsf         y.max=$b_buffer\n\n');

fprintf(fileID,'#TJ doping\n');
fprintf(fileID,'doping n.type uniform concentration=$TJ_d        y.min=$p_bsf         y.max=$p_TJ\n');
fprintf(fileID,'doping p.type uniform concentration=$TJ_d        y.min=$p_TJ          y.max=$n_TJ\n\n');

fprintf(fileID,'#Mesh for calculation of non-local tunneling current contribution\n');
fprintf(fileID,'#qtx.mesh location=0 spacing=1\n');
fprintf(fileID,'#qtx.mesh location=1 spacing=1\n');
fprintf(fileID,'#qty.mesh location=$p_TJ-0.9*$tp_TJ spacing=$tp_TJ/400\n');
fprintf(fileID,'#qty.mesh location=$p_TJ+0.9*$tp_TJ spacing=$tp_TJ/400\n\n');

fprintf(fileID,'#For the top section\n');
fprintf(fileID,'material mun=%6.2d ',InAlGaPwmu_n);
fprintf(fileID,'mup=%6.2d ',InAlGaPwmu_p);
fprintf(fileID,'region=1 \n');

fprintf(fileID,'material mun=%6.2d ',InGaPemu_n);
fprintf(fileID,'mup=%6.2d ',InGaPemu_p);
fprintf(fileID,'region=2 \n');

fprintf(fileID,'material mun=%6.2d ',InGaPbmu_n);
fprintf(fileID,'mup=%6.2d ',InGaPbmu_p);
fprintf(fileID,'region=3 \n');

fprintf(fileID,'material mun=%6.2d ',InAlGaPbsfmu_n);
fprintf(fileID,'mup=%6.2d ',InAlGaPbsfmu_p);
fprintf(fileID,'region=4 \n\n');

fprintf(fileID,'#For the tunnel junction\n');
fprintf(fileID,'material mun=1.0874e+03  mup=66.5026 region=5\n ');
% fprintf(fileID,'material mun=%6.2d ',1.0874e+03);
% fprintf(fileID,'mup=%6.2d ',66.5026);
% fprintf(fileID,'region=5 \n');

fprintf(fileID,'material mun=1.0874e+03  mup=66.5026 region=6\n\n ');
% fprintf(fileID,'mup=66.5026);
% fprintf(fileID,'region=6 \n\n');

% fprintf(fileID,'material mun=%6.2d ',GaAsTJpmu_n);
% fprintf(fileID,'mup=%6.2d ',GaAsTJpmu_p);
% fprintf(fileID,'region=6 \n\n');

fprintf(fileID,'#For the bottom section\n');
fprintf(fileID,'material mun=%6.2d ',InGaPwmu_n);
fprintf(fileID,'mup=%6.2d ',InGaPwmu_p);
fprintf(fileID,'region=7 \n');

fprintf(fileID,'material mun=%6.2d ',GaAsenmu_n);
fprintf(fileID,'mup=%6.2d ',GaAsenmu_p);
fprintf(fileID,'region=8 \n');

fprintf(fileID,'material mun=%6.2d ',GaAsbnmu_n);
fprintf(fileID,'mup=%6.2d ',GaAsbnmu_p);
fprintf(fileID,'region=9 \n');

fprintf(fileID,'material mun=%6.2d ',AlGaAsbsfmu_n);
fprintf(fileID,'mup=%6.2d ',AlGaAsbsfmu_p);
fprintf(fileID,'region=10 \n');

% fprintf(fileID,'material mun=%6.2d ',GaAsenmu_n);
% fprintf(fileID,'mup=%6.2d ',GaAsenmu_p);
% fprintf(fileID,'region=11 \n\n');

fprintf(fileID,'material mun=%6.2d ',GaAsbufnmu_n);
fprintf(fileID,'mup=%6.2d ',GaAsbufnmu_p);
fprintf(fileID,'region=11 \n\n');

fprintf(fileID,'contact name=tunnel resist=1e15\n\n');

fprintf(fileID,'material mat=InGaP   index.file=InGaP_ex.nk   \n');
fprintf(fileID,'material mat=AlGaAs  index.file=AlGaAs.nk     \n');
fprintf(fileID,'material mat=InAlGaP index.file=AlGaInP.nk\n\n');

fprintf(fileID,'material material=InGaP  affinity=$InGaP_aff\n');
fprintf(fileID,'material material=AlGaAs affinity=$AlGaAs_aff\n\n');

fprintf(fileID,'models print temperature=300 \n');
fprintf(fileID,'models srh conmob auger optr bgn fermi\n');
fprintf(fileID,'#model bbt.nonlocal bbt.nlderivs\n');

fprintf(fileID,'method newton #maxtraps=50\n');
fprintf(fileID,'output con.band val.band charge opt.intens \n\n');

fprintf(fileID,'beam num=1 AM0 x.origin=0.5 y.origin=-1.0 angle=90\n\n');

fprintf(fileID,'solve init\n');
fprintf(fileID,'save outfile=equilibriumSimpleTJ%d.str\n\n',i);

fprintf(fileID,'solve b1=0.9\n\n');

fprintf(fileID,'save outf=shortcircuitSimpleTJ%d.str\n\n',i);

fprintf(fileID,'log outfileTJ=forward_IVSimpleTJ%d.log\n',i);
fprintf(fileID,'solve name=Emitter vEmitter=0.0 vstep=0.05 vfinal=0.2\n\n');

fprintf(fileID,'save outfile=for_02SimpleTJ%d.str\n\n',i);

fprintf(fileID,'solve name=Emitter vEmitter=0.2 vstep=0.01 vfinal=3.5\n');
fprintf(fileID,'log off\n\n');

fprintf(fileID,'save outfile=forSimpleTJ%d.str\n\n',i);

fprintf(fileID,'quit\n\n');

fclose(fileID);

end
```

APPENDIX W.   MODEL DECKBUILD FILE

```
go ATLAS simflags = "-P 2"

#solar top section cell thicknesses set
set tp_window  =  0.03
set tp_emitter =  0.05
set tp_base    =  0.55
set tp_BSF     =  0.03

#solar top section cell doping concentrations set
set windowp_d  = 2e+18
set emitterp_d = 2e+18
set basep_d    = 7e+16
set BSFp_d     = 2e+18

#Top section mole compositions & affinity settings
set wp_comp    = 0.49
set bsfp_comp  = 0.7
set InGaP_aff  = 3.87
set AlGaAs_aff = 3.81

#solar cell TJ
set tp_TJ =  0.03
set TJ_d  = 2e+19

set p_window   = $tp_window
set p_emitter  = $p_window+$tp_emitter
set p_base     = $p_emitter+$tp_base
set p_bsf      = $p_base+$tp_BSF

set p_TJ       = $p_BSF+$tp_TJ
set n_TJ       = $p_TJ+$tp_TJ

#solar bottom section cell thicknesses set
set tb_window  =  0.04
set tb_emitter =  0.50
set tb_base    =  2.05
set tb_BSF     =  0.10
set tb_buffer  =  0.20

#solar bottom section cell doping concentrations set
set windowb_d  = 3e+18
set emitterb_d = 2e+18
set baseb_d    = 2e+17
set BSFb_d     = 2e+18

set bufferb_d  = 2e+18

#Bottom section mole compositions & affinity settings
set wb_comp    = 0.49
set bsfb_comp  = 0.7

set b_window   = $n_TJ+$tb_window
set b_emitter  = $b_window+$tb_emitter
set b_base     = $b_emitter+$tb_base
set b_bsf      = $b_base+$tb_BSF
set b_buffer   = $b_bsf+$tb_buffer

mesh
x.mesh location=0               spacing=1
x.mesh location=1               spacing=1
y.mesh location=0               spacing=$tp_window/20
y.mesh location=$p_window       spacing=$tp_window/20
y.mesh location=$p_emitter      spacing=$tp_emitter/100
y.mesh location=$p_base         spacing=$tp_base/5
y.mesh location=$p_bsf          spacing=$tp_BSF/100

y.mesh location=$p_TJ           spacing=$tp_TJ/20
y.mesh location=$n_TJ           spacing=$tp_TJ/20

y.mesh location=$b_window       spacing=$tb_window/20
y.mesh location=$b_emitter      spacing=$tb_emitter/100
y.mesh location=$b_base         spacing=$tb_base/5
y.mesh location=$b_bsf          spacing=$tb_BSF/100
y.mesh location=$b_buffer       spacing=$tb_buffer/100

#Top Section
region num=1 material=InAlGaP x.min=0 y.min=0 x.max=1    y.max=$p_window   x.comp = 0.371 y.comp = 0.159
region num=2 material=InGaP   x.min=0 y.min=$p_window    y.max=$p_emitter  x.comp=0.49
region num=3 material=InGaP   x.min=0 y.min=$p_emitter   y.max=$p_base     x.comp=0.49
region num=4 material=InAlGaP x.min=0 y.min=$p_base      y.max=$p_bsf      x.comp = 0.371 y.comp = 0.159

#tunnel junction
region num=5 material=GaAs x.min=0 x.max=1 y.min=$p_bsf y.max=$p_TJ
region num=6 material=GaAs x.min=0 x.max=1 y.min=$p_TJ  y.max=$n_TJ

#Bottom Section
```

```
region num=7  material=InGaP  x.min=0  y.min=$n_TJ       y.max=$b_window x.comp=0.49
region num=8  material=GaAs   x.min=0  y.min=$b_window   y.max=$b_emitter
region num=9  material=GaAs   x.min=0  y.min=$b_emitter  y.max=$b_base
region num=10 material=AlGaAs x.min=0  y.min=$b_base     y.max=$b_bsf    x.comp=0.7
region num=11 material=GaAs   x.min=0  y.min=$b_bsf      y.max=$b_buffer

electrode name=Emitter  top
electrode name=tunnel   x.min=0 x.max=1 y.min=$p_bsf y.max=$n_TJ material=GaAs
electrode name=Base     bottom

#For the top section
doping p.type uniform concentration=$windowp_d   y.min=0              y.max=$p_window
doping p.type uniform concentration=$emitterp_d  y.min=$p_window      y.max=$p_emitter
doping n.type uniform concentration=$basep_d     y.min=$p_emitter     y.max=$p_base
doping n.type uniform concentration=$BSFp_d      y.min=$p_base        y.max=$p_bsf

#For the bottom section
doping p.type uniform concentration=$windowb_d   y.min=$p_bsf         y.max=$b_window
doping p.type uniform concentration=$emitterb_d  y.min=$b_window      y.max=$b_emitter
doping n.type uniform concentration=$baseb_d     y.min=$b_emitter     y.max=$b_base
doping n.type uniform concentration=$BSFb_d      y.min=$b_base        y.max=$b_bsf
doping n.type uniform concentration=$bufferb_d   y.min=$b_bsf         y.max=$b_buffer

#TJ doping
doping n.type uniform concentration=$TJ_d        y.min=$p_bsf         y.max=$p_TJ
doping p.type uniform concentration=$TJ_d        y.min=$p_TJ          y.max=$n_TJ

#For the top section
material mun=1.06e+02 mup=5.10e+01 region=1
material mun=4.05e+02 mup=6.69e+01 region=2
material mun=6.76e+02 mup=1.52e+02 region=3
material mun=1.06e+02 mup=5.10e+01 region=4

#For the tunnel junction
material mun=1.32e+03 mup=8.33e+01 region=5
material mun=1.32e+03 mup=8.33e+01 region=6

#For the bottom section
material mun=3.64e+02 mup=5.53e+01 region=7
material mun=2.29e+03 mup=1.48e+02 region=8
material mun=3.91e+03 mup=2.42e+02 region=9
material mun=3.98e+02 mup=5.43e+01 region=10
material mun=2.29e+03 mup=1.48e+02 region=11

contact name=tunnel resist=1e15

material mat=InGaP   index.file=InGaP_ex.nk
material mat=AlGaAs  index.file=AlGaAs.nk
material mat=InAlGaP index.file=AlGaInP.nk

material material=InGaP  affinity=$InGaP_aff
material material=AlGaAs affinity=$AlGaAs_aff

models print temperature=300
models srh conmob auger optr bgn fermi
method newton
output con.band val.band charge opt.intens

beam num=1 AM0 x.origin=0.5 y.origin=-1.0 angle=90

solve init
save outfile=equilibrium.str

solve b1=0.9

save outf=shortcircuit.str
tonyplot shortcircuit.str

log outfileTJ=forward_IV.log
solve name=Emitter vEmitter=0.0 vstep=0.05 vfinal=0.2

save outfile=for_02.str

solve name=Emitter vEmitter=0.2 vstep=0.01 vfinal=3.5
log off

save outfile=for.str
tonyplot equilibrium.str for.str for_02.str
tonyplot forward_IV.log

quit
```

APPENDIX X. MATLAB EXECUTES DECKBUILD

```
function run_deckbuildPC(N)
%The purpose of this function is to execute deckbuild directly from
%MATLAB via the command line syntax for PC.  This function makes use of
%the doping concentration vector, N, in order to ensure all designs are
%executed

fprintf('Progress:\n');
fprintf(['\n' repmat('.',1,length(N(:,1))) '\n\n']);

for j=1:length(N(:,1))
%     command=sprintf("deckbuild -run -ascii test%dTJ.in",j);
    command=sprintf("deckbuild -run test6_%dTJ.in",j);
    [x,y]=system(command);
    fprintf('\b|\n');

end

**********************************************************************

function run_deckbuild(N)
%The purpose of this function is to execute deckbuild directly from
%MATLAB via the command line syntax for Linux.  This function makes use
%of the doping concentration vector, N, in order to ensure all designs
%are executed

fprintf('Progress:\n');
fprintf(['\n' repmat('.',1,length(N(:,1))) '\n\n']);

parfor j=1:length(N(:,1))
%     command=sprintf("deckbuild -run -ascii test%dTJ.in",j);
    command=sprintf("deckbuild -run -ascii test6_%dTJ.in",j);
    [x,y]=system(command);
    fprintf('\b|\n');

end
```

THIS PAGE INTENTIONALLY LEFT BLANK

APPENDIX Y. CURVE FITTING AND PROBABILITY ANALYSIS

```
function [Ex_thick, Ex_doping] = findRange(N,design_thickness,eff)
% The purpose of this function is to produce a usable range for new design
% parameters in respect to thickness and doping
%
%  [Ex_thick, Ex_doping] = findRange(N,design_thickness,eff)

N_log=log10(N);            %strips the exponential value for the doping concentration
thick_x=design_thickness; %reassigns thickness to a maneagable variable for implementation below
doping_x=N_log;            %reassigns doping to a maneagable variable for implementation below

for i=1:length(N(1,:))
   func_thick(:,i)    = polyfit(design_thickness(:,i),eff',2);  %develops a + bx +cx^2 for thickness
   func_doping(:,i)   = polyfit(N_log(:,i),eff',2);             %develops a + bx +cx^2 for doping
   max_thick(:,i)     = polyval(func_thick(:,i),eff',2);        %finds maximums for thickness
   max_doping(:,i)    = polyval(func_doping(:,i),eff',2);       %finds maximums for doping
   fmax_thick(:,i)    = max(max_thick(:,i));                    %finds actual maximum for thickness
   fmax_doping(:,i)   = max(max_doping(:,i));                   %finds actual maximum for doping

   %% Expressions and functions for thickness
   thick_x0_x1(:,i) = thick_x(end,i)-thick_x(1,i);              %performs x1 - x0 for thickness
   thick_abc(:,i)=func_thick(1,i)*(thick_x0_x1(i)) + 1/2*func_thick(2,i)*(thick_x0_x1(i)).^2 + 1/3*func_thick(3,i)*(thick_x0_x1(i)).^3;
   %Caculates individual poritons for E(x) for portions 1, 2, and 3 from
   %the hand calculations for thickness
   forT_a(:,i)      =1/3*(thick_x0_x1(i)).^3 -(thick_x0_x1(i)).^2.*fmax_thick(i) + (thick_x0_x1(i)).*fmax_thick(i).^2;
   forT_b(:,i)      =1/4*(thick_x0_x1(i)).^4 -2/3*(thick_x0_x1(i)).^3.*fmax_thick(i) + 1/2*thick_x0_x1(i).^2.*fmax_thick(i).^2;
   forT_c(:,i)      =1/5*(thick_x0_x1(i)).^5 -1/2*thick_x0_x1(i).^4.*fmax_thick(i) + 1/3*(thick_x0_x1(i)).^3.*fmax_thick(i).*2;
   %Calculating the entirety of the portions 1, 2, and 3 with the
   %coefficients a, b, and c for thickness
   thick_exp(:,i)    =func_thick(1,i).*forT_a(i) + func_thick(2,i).*forT_b(i) + func_thick(3,i).*forT_c(i);

   %% Expressions and functions for doping
   doping_x0_x1(:,i) = doping_x(end,i)-doping_x(1,i);           %performs x1 - x0 for doping
   doping_abc(:,i)   = func_doping(1,i).*(doping_x0_x1(i)) + 1/2*func_doping(2,i).*(doping_x0_x1(i)).^2 + 1/3*func_doping(3,i).*(doping_x0_x1(i)).^3;
   %Caculates individual poritons for E(x) for portions 1, 2, and 3 from
   %the hand calculations for doping
   forD_a(:,i)      =1/3*(doping_x0_x1(i)).^3 -(doping_x0_x1(i)).^2.*fmax_doping(i) + (doping_x0_x1(i)).*fmax_doping(i).^2;
   forD_b(:,i)      =1/4*(doping_x0_x1(i)).^4 -2/3*(doping_x0_x1(i)).^3.*fmax_doping(i) + 1/2*doping_x0_x1(i).^2.*fmax_doping(i).^2;
   forD_c(:,i)      =1/5*(doping_x0_x1(i)).^5 -1/2*doping_x0_x1(i).^4.*fmax_doping(i) + 1/3*(doping_x0_x1(i)).^3.*fmax_doping(i).*2;
   %Calculating the entirety of the portions 1, 2, and 3 with the
   %coefficients a, b, and c for doping
   doping_exp(:,i)  =func_doping(1,i).*forD_a(i) + func_doping(2,i).*forD_b(i) + func_doping(3,i).*forD_c(i);

   %% Calculates the entirety of E(x) for both thickness and doping
   Ex_thick(:,i)    =1./thick_abc(i).*(thick_exp(i));
   Ex_doping(:,i)   =1./doping_abc(i).*(doping_exp(i));

end

end
```

THIS PAGE INTENTIONALLY LEFT BLANK

LIST OF REFERENCES

[1] J. S. Walsh, "Optimization of multi-junction solar cells for space applications modeled with Silvaco ATLAS," M. S. thesis, Dept. Elec. Eng., NPS, Monterey, CA, USA, 2018. [Online]. Available: http://hdl.handle.net/10945/59615

[2] P. Michalopoulos, "A novel approach for the development and optimization of state-of-the-art photovoltaic devices using Silvaco," M. S. thesis, Dept. Elec. Eng, NPS, Monterey, CA, USA, 2003. [Online]. Available: https://calhoun.nps.edu/handle/10945/5609

[3] R. Kilway, "Five-junction solar cell optimization using Silvaco ATLAS," Dept. Elec. Eng., NPS, Monterey, CA, USA, 2017. [Online]. Available: https://calhoun.nps.edu/handle/10945/56146

[4] S. Pueschel, "Optimization of an advanced multi-junction solar-cell design for space environments (AM0) using nearly orthogonal Latin hypercubes," M. S. thesis, Dept. Op. Res., NPS, Monterey, CA, USA, 2017. [Online]. Available: http://hdl.handle.net/10945/55521

[5] B.G. Streetman and S. K. Banerjee, *Solid State Electronic Devices*, Upper Saddle River, NJ, USA: Prentice-Hall , 2009.

[6] M. Lundstrom, "Introduction to Photovoltaics," class notes for NCN Summer School, Purdue University, West Lafayette, IN, USA , 2011. [Online]. Available https://nanohub.org/resources/11884/download/2011.07.20-NCN-SC01-Lundstrom.pdf

[7] S. M. Sze and K. K. Ng, *Physics of Semiconductor Devices*, Hoboken, NJ, USA: John Wiley and Sons , 2007.

[8] M. R. Lueck, C. L. Andre, A. J. Pitera, M. L. Lee, A. Fitzgerald, and S. A. Ringel, "Dual-junction GaInP/GaAs solar cells grown on metamorphic SiGe/Si substrates with high open circuit voltage," *IEEE Electron Device Letters*, vol. 27, no. 3, pp. 142–144, 2006.

[9] A. D. MacCalman, H. Vieira, and T. Lucas, "Second-order nearly orthogonal Latin hypercubes for exploring stochastic simulations," *Journal of Simulation*, vol. 11, no. 2, pp. 137–150, May 2017.

[10] RubyInstaller. 2019. [Online] Available: https://rubyinstaller.org/

THIS PAGE INTENTIONALLY LEFT BLANK

INITIAL DISTRIBUTION LIST

1. Defense Technical Information Center
   Ft. Belvoir, Virginia

2. Dudley Knox Library
   Naval Postgraduate School
   Monterey, California